INVESTIGATION OF CLOUD PROPERTIES AND ATMOSPHERIC PROFILES WITH MODIS

SEMI-ANNUAL REPORT FOR JANUARY – JUNE 2003

Paul Menzel, Steve Ackerman, Chris Moeller, Liam Gumley, Richard Frey, Jun Li,
Bryan Baum, Jeff Key, Suzanne Seemann, Tom Rink, Kathy Strabala,
Hong Zhang, and Dan LaPorte.
CIMSS at the University of Wisconsin-Madison

Contract NAS5-31367

ABSTRACT

UW assessed Aqua MODIS L1B thermal infrared band radiometric accuracy using ER-2 based observations collected during TX-2002; it was found that most Aqua MODIS bands are performing within or very near specification. UW also participated in the THORpex OST (TOST) field experiment in February/March wherein the ER-2 underflew Aqua collecting data sets for assessing Aqua MODIS L1B and cloud product accuracy. A new destriping algorithm for MODIS Level-1B 1 km image data was successfully tested; it is based on matching empirical distribution functions suggested in Weinreb et al. and greatly improves some products, especially the IR based cloud phase and total precipitable water vapor (TPW). UW continued tuning the algorithms for cloud mask, cloud top properties, and atmospheric profiles (MOD35, MOD06, and MOD07); updates incorporate radiance bias adjustments and improved treatment of surface emissivity and skin temperature in the training datasets. TPW is much improved in drier atmospheres and over surfaces with non-black emissivities such as deserts, grassland, and other less vegetated surfaces. A daytime multi-layered cloud detection methodology is being applied to MODIS direct broadcast data at CIMSS and will be tested in the cloud top pressure algorithm. An effort to improve the characterization of the surface via clear-sky radiance maps has been active. A set of web pages of UW MODIS research has been developed. Operational use of polar winds at the European Center for Medium range Weather Forecast started January 2003 and the NASA Data Assimilation Office and the US Navy Fleet Numerical Meteorology and Oceanography Center continued assimilation impact studies. The International MODIS and AIRS Processing Package IMAPP Level 2 science product Version 1.3 was released in first quarter 2003; it included updates to the cloud mask (MOD35) and cloud top property (MOD06CT) software which allows both Aqua and Terra data to be processed. Aqua MODIS and AIRS data were combined to investigate the cloudiness within an AIRS pixel. Seven MODIS articles were published (two in the Journal of Applied Meteorology, three in IEEE Transactions on Geoscience and Remote Sensing, two in Journal of Geophysical Research). The EOS Data Products Handbook with more current references and product examples was updated. Three conference papers were given and a training session was conducted in Italy.

TASK OBJECTIVES

MODIS Infrared Calibration

Aqua MODIS L1B radiometric accuracy for TIR bands was assessed using ER-2 based observations collected during TX-2002. These show that most Aqua MODIS bands are performing within or very near specification. The Aqua MODIS destriping coefficients for band

26 was generated and delivered to MCST for use in the MODIS L1B product algorithm. As part of the THORpex OST (TOST), the ER-2 underflew Aqua in the February/March timeframe collecting data sets useful for assessing Aqua MODIS L1B and cloud product accuracy.

MODIS Cloud Mask (MOD35)

An adjustment was made to the Aqua snow detection algorithm. Previously, band 7 (2.1 μm) reflectances were substituted for those of band 6 (1.6 μm) due to the poor quality of the latter. During the winter (2002-2003) months, it became obvious that a band 7 threshold set in autumn 2002 was not adequate for winter conditions in the far north. In addition, a 3.75-11 μm brightness temperature difference (BTD) test was added to the 8.5-11 μm BTD test. A refinement of the smoke detection algorithm has been tested and will be included in Collection 5 processing. Clear-sky radiance data from MODIS were compared to that from AVHRR generated from the CLAVR (Clouds from AVHRR) cloud screening algorithm, while cloud frequencies from MODIS were compared to ground-based lidar data. A study of the effects on clear-sky detection and clear vs. cloudy radiance data at various field of view (FOV) sizes and sampling frequencies has begun. MODIS cloud mask and 1-km radiance information were used to simulate measurements from instruments with various footprint sizes.

MODIS Cloud Top Properties (MOD06)

A change was made to the MODIS Atmosphere Level 3 algorithm where daily, 8-day, and monthly statistics are accumulated. Cloud top temperatures as low as 190K are now reported in order to describe the very cold clouds associated with deep convective systems. Monthly values of high cloud frequency from MODIS were compared to those from ISCCP and HIRS. In addition, cloud statistics from Terra and Aqua MODIS were compared for overall consistency and expected diurnal differences.

MODIS Infrared Total Precipitable Water Product (MOD07)

A new version of the operational MOD07 product code was delivered in June 2003. Errors related to radiance bias corrections (including a discontinuity in retrievals at latitude 50N, a dry bias in TPW retrievals for moist cases, and surface emissivity effects) and difficulties caused by using the difference between two short wavelength infrared bands (25-24) as a predictor (especially from detector to detector striping) were corrected.

Polar Winds

Real-time MODIS polar winds continue to be generated from both Terra and Aqua. MODIS level 1b granules for both polar regions are obtained through the NOAA “bent pipe”. Approximately 200 granules per day (50 GB) are transferred via FTP from a NOAA computer at Goddard Space Flight Center to CIMSS. Wind retrievals are then done locally and made available to the scientific community via anonymous FTP within 3-6 hours after MODIS views any given area. A major milestone was reached in January when the European Centre for Medium Range Weather Forecasts (ECMWF) began including the MODIS polar winds in their operational forecast system. The NASA Data Assimilation Office (DAO) continues to use the winds in their experimental forecasting system. Additionally, CIMSS now routinely transfers the real-time winds data to the Fleet Numerical Meteorology and Oceanography Center (FNMOC, U.S. Navy), where they are being tested in the FNMOC 3-dimensional variational analysis

(3DVAR) system. Real-time MODIS wind plots are available on the Web at http://stratus.ssec.wisc.edu/products/rtpolarwinds.

Realtime Aqua Processing

After obtaining the current version of the AIRS/AMSU/HSB Level-1 processing package for direct broadcast use, SSEC is working with JPL to beta test the package prior to release to the international community. In May 2003, SSEC began near real-time production of AIRS/AMSU/HSB Level-1 data using locally acquired direct broadcast data. Distribution is restricted to SSEC and JPL until beta testing of the software is complete.

Study on the synergistic use of MODIS cloud products and AIRS radiance measurements

Synergistic use of MODIS high spatial resolution cloud products and high spectral resolution AIRS radiance measurements from Aqua were studied with the goal of achieving optimal retrieval of atmospheric profile and cloud parameters. The collocated MODIS cloud products (cloud mask, surface and cloud types, cloud phase, cloud-top pressure, effective cloud amount, cloud particle size, liquid water path, ice water path) and AIRS cloudy radiance measurements can be used for retrieving improved cloud products. The study has the goal of improving cloud parameters retrieved from AIRS cloudy radiance measurements with a variational (1DVAR) algorithm using MODIS cloud products as the background and first guess information.

WORK ACCOMPLISHED

MODIS Infrared Calibration

During the Terra-Aqua experiment – 2002 (TX-2002), a NASA ER-2 gathered collocated data with the EOS Aqua satellite over the Gulf of Mexico for the purpose of gaining insight on the accuracy of MODIS thermal infrared (TIR) band radiances. The ER-2 payload included the MODIS Airborne Simulator (MAS) and the Scanning High resolution Interferometer Sounder (SHIS). The ER-2 based MAS observations were used to simulate top-of-atmosphere (TOA) radiances for MODIS. MODIS viewed the target region at nadir during the overpass. The MAS observations were adjusted to the spectral, spatial, and altitude characteristics of MODIS to rigorously simulate MODIS on-orbit data. Atmospheric slant path dependence was removed by matching the MAS slant path viewing geometry to that of MODIS (+/- 3°) observations. The SHIS data set provides radiometrically accurate (conservatively estimated to be less than 0.5°C) TIR band radiances for a calibration transfer to MAS observations, and a means to spectrally correct MAS data to MODIS spectral characteristics using real observations, i.e. the SHIS high spectral resolution data.

MODIS residuals averaged over all detectors of each band are given in Table CCM1 and shown in Figure CCM1 along with the MODIS radiometric accuracy specification. The MODIS ozone sensitive band 30 is not included in the results because no reliable ozone profile was available for November 21. Past experience has shown that climatological ozone profiles do not provide sufficiently accurate characterization to assess that band. Most MODIS bands are within or very near specification. Exceptions include MODIS band 20 and band 25. Given the presence of sunglint, the band 20 result is disregarded. The MODIS band 25 result bears further investigation. Residuals in bands 33 – 36 were further investigated due to the uncertainty in the atmospheric correction. A 2nd radiosonde (Lake Charles, LA; 1200 UTC on November 21) was

used to produce an atmospheric correction. Figure CCM2 shows the altitude correction comparison using the chosen Corpus Christi TX profile and the Lake Charles LA profile; only modest (0.1 to 0.2°C) sensitivity is evident for bands 25, 33, and 34 but larger sensitivity for band 35 (0.5°C) and 36 (0.9°C). As a result, the residuals for bands 35 and 36 are considered less reliable (see RSS of Uncertainties in Table CCM1).

Table CCM1. MODIS detector averaged residuals for November 21, 2001. Shaded entries are within or very nearly within MODIS radiometric accuracy specification. AOI is MODIS scan mirror angle of incidence (38° for nadir viewing). "*" indicates atmospheric band.

MODIS Band Number	Central Wavelen (μm)	Spectral Correc-tion (K)	Spatial Correc-tion (K)	SHIS Cal Transfer (K)	Altitude Correc-tion (K)	MODIS Residual (K)	RSS of Uncer-tainty (K)	MODIS Accuracy Spec (K)
AOI	-	-	-	-	-	38°	-	
Samples	-	-	-	-	-	332	-	+/-
20	3.788	0.24	1.76	0.86	-0.02	-0.63	0.17	0.18
21	3.992	-0.11	1.22	0.57	-0.02	-0.74	0.17	3.00
22	3.972	-0.16	0.55	0.57	-0.03	-0.11	0.17	0.25
23	4.057	-1.21	-1.04	0.20	-0.04	0.07	0.16	0.25
24*	4.473	27.23	28.93	2.14	0.62	-0.19	0.35	0.19
25*	4.545	2.41	5.54	2.14	-0.12	-0.87	0.19	0.24
27*	6.765	-1.33	-0.20	1.43	0.12	0.18	0.22	0.27
28*	7.337	9.30	10.49	1.17	0.01	-0.03	0.18	0.32
29	8.541	-0.08	1.75	1.51	-0.29	-0.03	0.20	0.53
30*	9.730	1.41	10.65	1.21	-5.02	-3.01	2.24	0.42
31	11.014	0.01	1.97	1.81	0.00	-0.15	0.17	0.34
32	12.028	-0.10	2.03	1.98	-0.01	-0.13	0.17	0.37
33*	13.361	5.39	7.90	1.24	-0.55	-0.72	0.24	0.61
34*	13.679	-8.05	-6.72	1.43	-0.54	0.64	0.30	0.58
35*	13.911	2.83	3.08	1.43	0.26	0.93	0.59	0.55
36*	14.195	-5.03	-9.37	-1.61	1.89	0.84	0.87	0.47

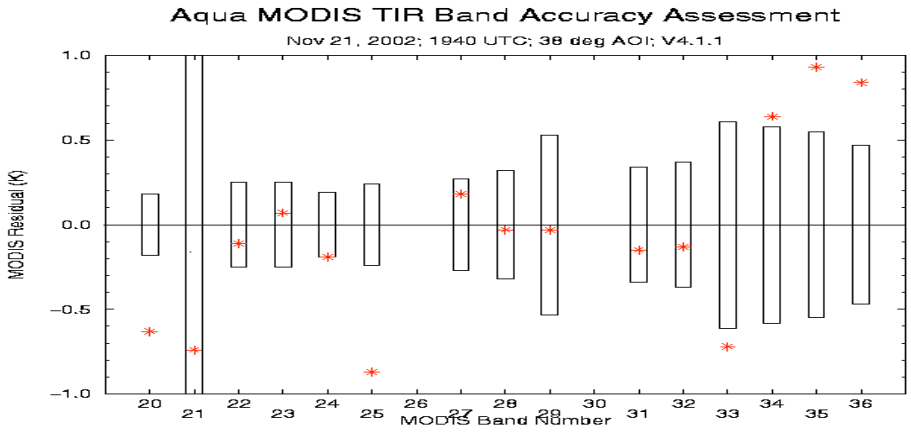

Figure CCM1. Aqua MODIS detector averaged residuals (stars) for 21 November 2002 over the Gulf of Mexico (295 K scene temperature at 11 μm). Positive residuals indicate MODIS L1B calibrated temperature is warmer than expected. The residuals for most spectral bands fall within the radiometric accuracy specification envelope (open bars). Sunglint affects band 20. Uncertainties (Table 2) suggest less confidence in band 24, 30 (not shown), 35 and 36 residuals.

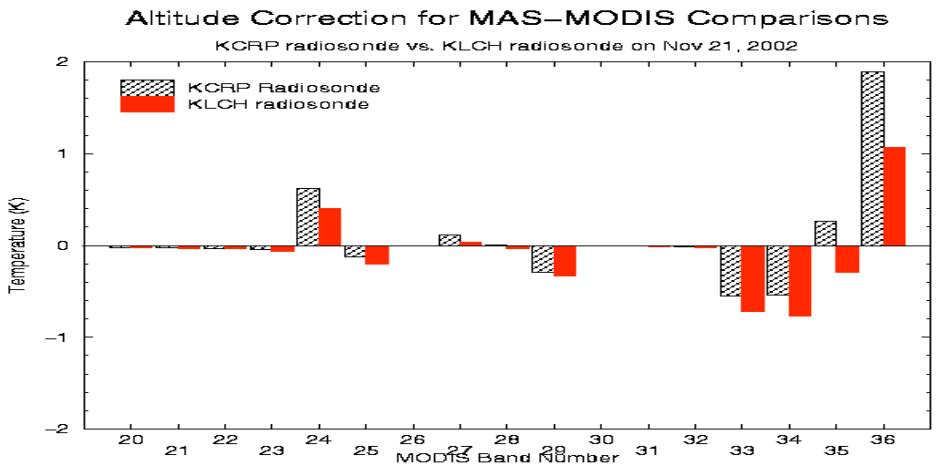

Figure CCM2. Altitude correction using Corpus Christi, TX (KCRP) and Lake Charles, LA (KLCH) radiosonde profiles. The altitude correction in MODIS bands 35 and 36 shows highest sensitivity of about 0.5°C and 0.9°C, respectively to the choice of radiosonde.

As with Terra MODIS, the Aqua MODIS band 31 and 32 residuals are small and slightly negative (cold). The close agreement in the band 31 and 32 residuals suggests that the radiometric bias will cancel in algorithms that use the split window difference. Aqua MODIS LWIR CO_2 sensitive bands (Bands 33-36) show smaller residuals than those of Terra MODIS, which showed residuals in excess of 1.78°C and 2.23°C for bands 35 and 36 respectively. The data quality of the Aqua MODIS LWIR CO_2 sensitive bands is also much improved. Terra MODIS LWIR CO_2 sensitive bands are known to be influenced by an optical light leak from the band 31 (11 μm) spectral region; a correction algorithm has been tested and implemented.

To gain insight on Aqua MODIS detector-to-detector striping, the MAS-MODIS residuals were also calculated for each of the ten MODIS detectors per TIR band. The 332 samples used in the MODIS residuals were sorted by detector to obtain the detector specific residuals. Figure CCM3 presents the results for a sample of MODIS TIR bands. These show some evidence of striping. For example, band 29 (8.52 μm) detector 1 (product order) is about 0.25°C cooler than other detectors in the November 21 data set assessment. Several bands (20, 28, 34, 35) show variation from detector to detector of about 0.20°C. Striping appears to be below 0.10°C for band 31 (11.01 μm) and 32 (12.02 μm). There appears to be correlation in the striping between bands 34 and 35. Detector striping is expected to be a function of scene temperature and instrument operating conditions. Thus the findings in this assessment should not be considered applicable as a correction to other MODIS data. Additionally, the sample size is relatively small.

The uncertainty associated with the MODIS accuracy assessment rests largely on the SHIS radiometric accuracy and the altitude correction. Uncertainties associated with other factors such as co-location error and temporal change are estimated to be 0.10°C or less. The altitude correction uncertainty based on the change in altitude correction using two different atmospheric characterizations is negligible for window bands but is important for upper atmospheric CO_2 sensitive bands. For MODIS band 36 in particular, the atmospheric correction uncertainty is on the order of 1°C, and for band 35 it is near 0.50°C. For other atmospheric bands it is < 0.5°C.

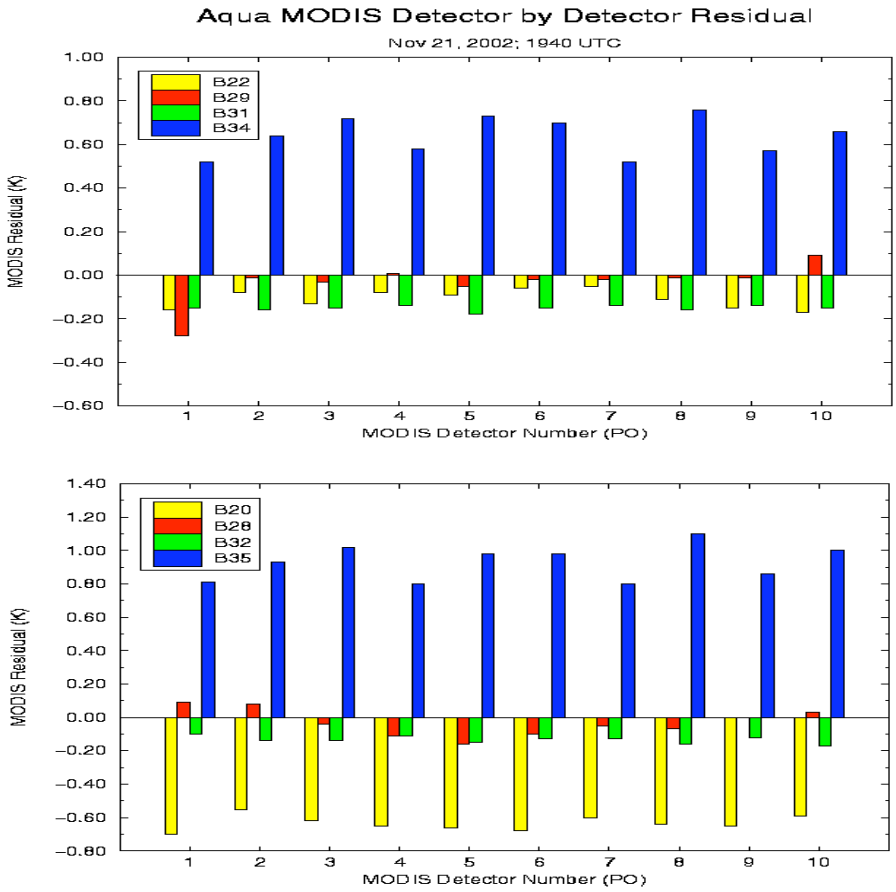

Figure CCM3. MODIS residuals given by detector for MODIS bands 22 (3.97 μm), 29 (8.52 μm), 31 (11.01 μm) and 34 (13.68 μm) (top panel) and bands 20 (3.79 μm), 28 (7.34 μm), 32 (12.02 μm) and 35 (13.91 μm) (bottom panel). Some striping is evident in many bands. For example, about 0.25°C in detector 1 (product order) of band 29 and about 0.20°C in several detectors of band 34. Striping in the LWIR split window bands 31 and 32 is below 0.10°C. These results are obtained from a relatively small sample size of 33 comparisons per detector.

The SHIS radiometric performance is closely related to the performance of the two high emissivity (.999, known to within .001) onboard blackbody cavities and to the non-linearity of the system. The radiometric uncertainty of the SHIS data was estimated using the expected blackbody performance uncertainty of 0.10°C in temperature, .001 in emissivity, and a 10% uncertainty in the nonlinear calibration term. The scene conditions and SHIS in-flight blackbody temperatures of November 21, 2002 were used for the analysis. The results of this analysis show that SHIS accuracy is about 0.10°C or less for all equivalent MODIS spectral bands except band 24 (0.24°C), band 27 (0.15°C), band 29 (0.13°C), band 34 (0.12°C), band 35 (0.16°C), and band 36 (0.26°C). These SHIS radiometric uncertainties indicate that all MODIS TIR bands can be assessed using SHIS. However, the root sum square (RSS) of the combined uncertainties (shown in Table CCM1) suggest that when other sources of uncertainty are included, particularly the altitude correction uncertainty, the assessment of bands 24, 30, 35, and 36 are challenged or not possible until the combined uncertainty can be reduced.

MAS IR Calibration Studies

MAS radiometric performance was evaluated through comparisons to SHIS using data from November 21, 2002. Findings of these comparisons suggest that MAS TIR band calibration offsets have increased (Figure CCM5), likely as a result of change in the onboard blackbody emissivity characteristics. At the recent (May, 2003) MAS instrument meeting it was suggested that the MAS onboard blackbodies be characterized in the near term, and consideration be given to recoating the blackbodies to raise their emissivity closer to historical levels.

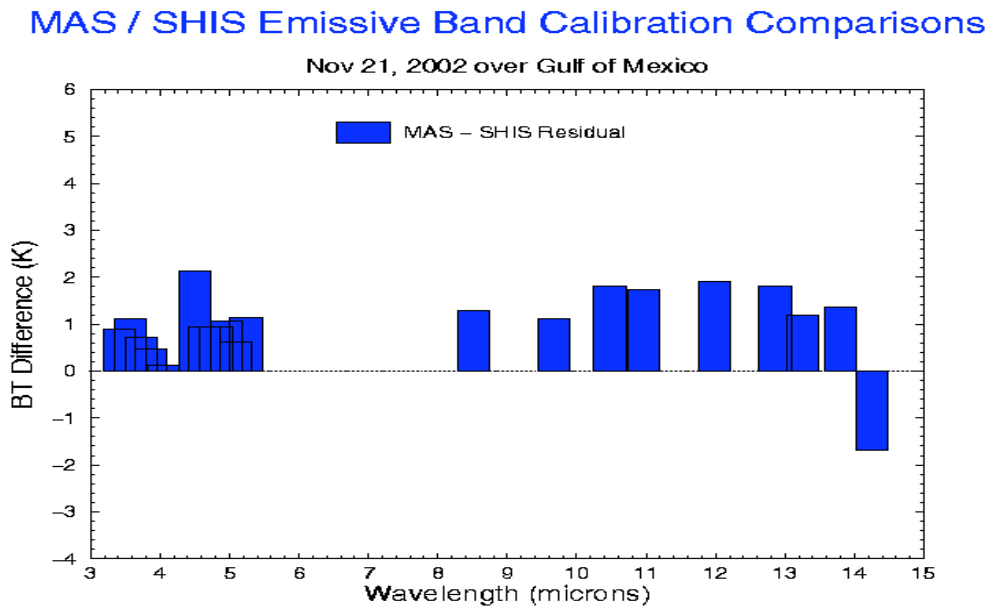

Figure CCM5. MAS-SHIS comparisons for 21 November 2002. MAS showed unexpectedly large residuals, especially in the LWIR window band region. These results suggest that the MAS blackbody emissivity has degraded over the last 1 to 2 years.

ER-2 MODIS Validation Activities

During the THORpex Observing System Test (TOST), the NASA ER-2 directly underflew Aqua during seven missions and crossed or flew very near to the Aqua orbital track on several others (Table CCM2). The scenes include daytime clear sky for L1B assessment, thin cirrus for cloud mask testing, single layer clouds for MODIS TIR band cloud phase product (MOD06) investigations, and multi-layer clouds for cloud height assessment. The MAS data set is now available at the GSFC archive in HDF format.

Table CCM2. NASA ER-2 flights during THORpex field Campaign.
February 18 – March 14, 2003

Date	Flt#	Sensor	Region	Comments
02/18				Scheduled ferry mission canceled for ER-2 aircraft issues.
02/19	6013	M,N,S,C	CA to HI	***Ferry flight***. Low OVC, subtropical cirrus, then low OVC. Crossed Aqua track at 2110 UTC (Aqua at 2157 UTC).
02/20				Down day for orientation, etc. Pleasant day in HI.
02/21	6014	M,N,C,S	40 N	***THORpex Jet Stream characterization mission***. Partial data due to ER-2 panel failure. Strong O3 gradient at jet position.
02/22	6015	M,N,C,S	E of HI	***THORpex Jet Stream characterization mission w/G4.*** Subtropical jet cirrus w/G4 profiling and dropsondes.
02/23				Planned No-Fly day. Warm day in HNL
02/24	6016	M,N,C,S	35 N	***Aqua Cloud validation mission***. Expansive multi-layer cloud in midlatitude wave. Aqua at 2355 UTC (nadir).
02/25				Flight canceled to allow instrument teams to work issues.
02/26	6017	M,N,C,S	30 N	***Aqua Cloud validation and GLAS validation mission***. Thin to thick multilayer cloud (high, mid, low level). Aqua at 2342 UTC (39° sat view angle). ICESat at nadir.
02/27				Hard down day for crew rest. Warm (80s) in HNL.
02/28				No fly day for ER-2 maintenance.
03/01	6018	M,N,C,S	22 N	***Aqua L1B/atmos. profiles and GLAS validation mission***. P/C skies with low clouds under Aqua (0010 UTC, nadir) and ICESat (0154 UTC, nadir). G-4 dropsondes.
03/02				No-fly day. ER-2 aircraft hydraulic leak repaired
03/03	6019	M,N,C,S	20 N	***Aqua L1B/Atmos. Profiles validation mission*** **w/G-4** dropsondes. Aqua (nadir) at 2358 UTC; mostly clear sky
03/04				ER-2 down for hydraulilc leak on NASA 806.
03/05				ER-2 down for hydraulic leak
03/06				ER-2 down for hydraulic leak
03/07				ER-2 down for hydraulic leak
03/08				ER-2 down for hydraulic leak
03/09				NASA 809 arrives in HNL to replace 806. Instruments uploaded to 809.
03/10	9031	M,N,C,S	33 N	***Aqua and ICESat cloud validation mission.*** Aqua (nadir, 0007 UTC) and ICESat (0144 UTC) with multi-layer cloud.
03/11	9032	M,N,C,S	32 N	***GIFTS Data Cube mission w/G-IV***. Clear and undercast in the data cube region. Aqua at 2311 UTC.
03/12	9033	M,N,C,S	41 N	***THORpex Jet Stream characterization mission w/G-IV.*** Transect strong Jet. Aqua at 2357 UTC (nadir). P/C skies.
03/13	9034	M,N,C,S	HI	***Atmospheric Moisture Winds***. UNH lidar coordination. Kileaua vent overflight. Clear sky scenes for wind estimates.
03/14	9035	M,N,C,S	40 N to DFRC	***THORpex Jet Stream characterization mission w/G-IV***. Flew along strong Jet axis back to DFRC.

Sensor Legend: M = MAS; N = NAST-I/M; C = CPL; S = SHIS

MODIS Band 26 Destriping Studies

Coefficients to destripe and remove unexpected surface reflectance from Aqua MODIS band 26 data have been completed. The algorithm and coefficients are highly similar to those applied to Terra MODIS for band 26 destriping. The coefficients have been delivered to MCST for implementing in the L1B production code of Aqua MODIS.

Monitoring and evaluation of Terra MODIS band 26 destriping have continued. A global data set showing the impact of destriping and removal of unexpected surface reflectance in the band 26 radiances was analyzed. Histograms (Figure CCM4) of clear sky scenes (based on MOD35 cloud mask product) show the elimination of outlying radiances after correction, in agreement with expectations based on model studies. This indicates that the corrected band 26 radiances are improved in accuracy.

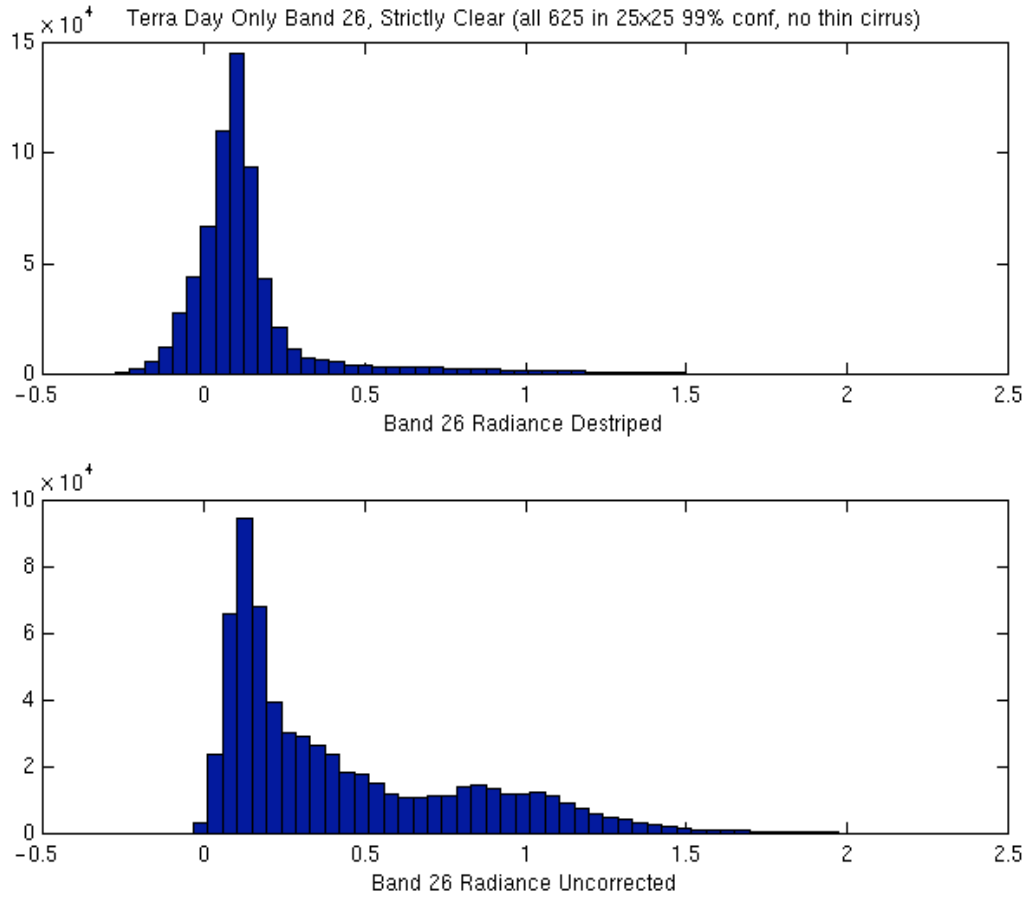

Figure CCM4. Terra MODIS Band 26 (1.38 μm) radiances for a global day of clear sky data. After the destriping correction (top) the global radiances take on a normal distribution. Before correction (bottom), the radiances strongly show the evidence of surface reflectance. Some surface reflectance is expected over dry regions of the globe; however, MODIS imagery has shown that uncorrected band 26 imagery includes surface reflectance over all global regions.

Destriping Algorithm for Thermal Emissive Bands

A new destriping algorithm for MODIS Level-1B 1 km image data was developed by Liam Gumley. The algorithm is based on Weinreb et al., 1989: "Destriping GOES Images by Matching Empirical Distribution Functions". Remote Sens. Environ., 29, 185-195. The algorithm accounts for both detector-to-detector and mirror side striping by treating MODIS as a 20-detector instrument in the emissive bands (10 detectors on each mirror side). The empirical distribution function (EDF) is computed for each detector (also known as the cumulative histogram of relative frequency). The EDF for each detector is then adjusted to match the EDF of a reference detector.

The prototype implementation of the algorithm is written in IDL, and requires fewer than 100 lines of code. The code operates on the scaled integers (0-32767) stored in the MOD021KM files and MYD021KM files, in DAAC or IMAPP format. A scaled integer correction LUT is created for each individual granule, and it takes about 60 seconds to process all the thermal infrared bands in each 5-minute granule. Uncorrected scaled integers are replaced with corrected scaled integers, however one could store the correction LUT instead. Bands 20, 22-25, 27-36 are destriped (impact on 31 and 32 is small, but significant for 8.5-11 and 11-12 micron difference). For Terra MODIS, the following noisy detectors are replaced with their neighbors: Band 27 (det 6); Band 28 (dets 0, 1); Band 33 (det 1); Band 34 (dets 6, 7, 8). For Aqua MODIS, no detectors are replaced. The algorithm is now applied routinely to MODIS data received by direct broadcast at SSEC and can be viewed at http://eosdb.ssec.wisc.edu/modisdirect/. Examples of the destriping algorithm applied to Terra and Aqua MODIS are shown in Figures LG1 and LG2.

SSEC expects to have this algorithm operational in time for Collection 5 reprocessing, either as part of the Level-1B calibration algorithm, or as part of the SSEC MODIS products. If the algorithm is not implemented as part of the Level-1B algorithm, it will mean that all reprocessed data archived at the DAAC will contain striping in the thermal emissive bands.

MODIS Visualization

New IDL software to visualize the SSEC MODIS clear radiance global grid at native resolution (i.e., one pixel in the display is one pixel in the grid) was developed by Liam Gumley. This allows the clear radiance grids to be inspected and debugged in detail. An example is shown in figure LG-3. The clear radiance grid is equal area and contains grid cells with dimensions 25 x 25 km. Normally the grids are stored as a linear array with 814880 elements, however it was discovered that the grids could be converted to a 1600 x 800 two-dimensional representation of a sinusoidal projection. It is felt that this software will prove indispensable for testing the clear radiance compositing routines under development for Collection 5 processing.

Band 2 (0.87 micron)

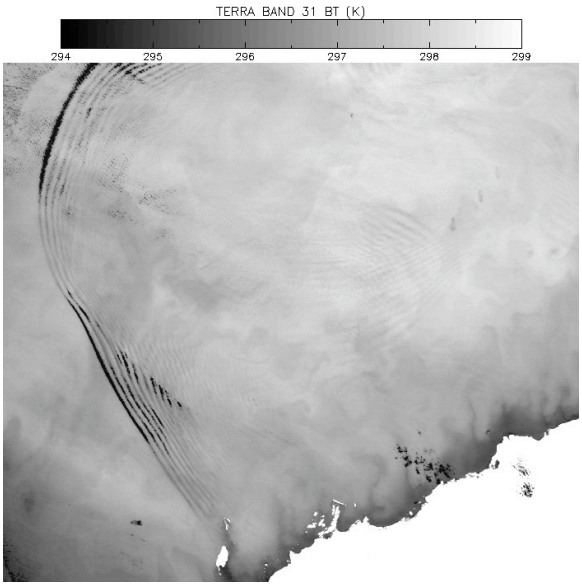

Band 31 (11.0 micron)

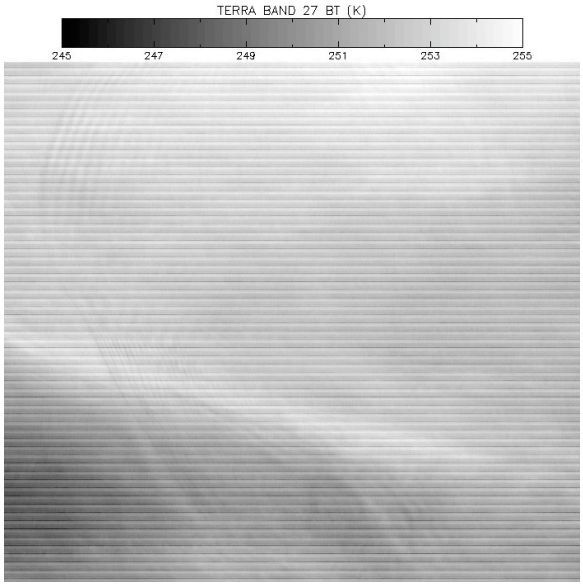

Band 27 (6.7 micron) original

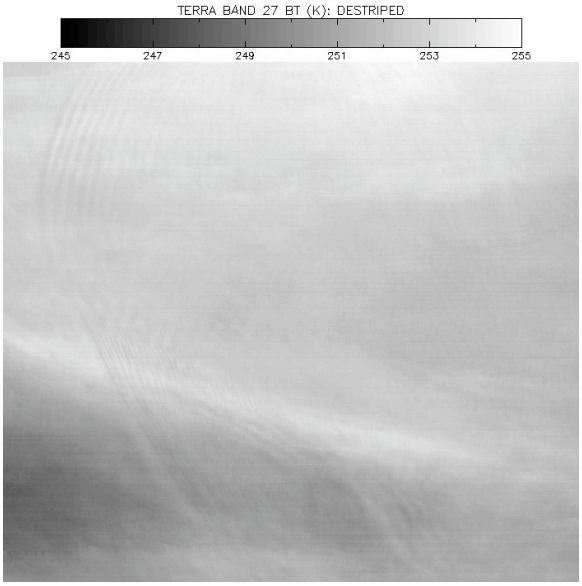

Band 27 (6.7 micron) destriped

Figure LG1. Example of Terra MODIS Destriping
MOD021KM.A2003146.0230.004.2003149043507.hdf (2003/05/26, 02:30 UTC)
Northwest Shelf of Western Australia, 700 x 700 pixel subscene

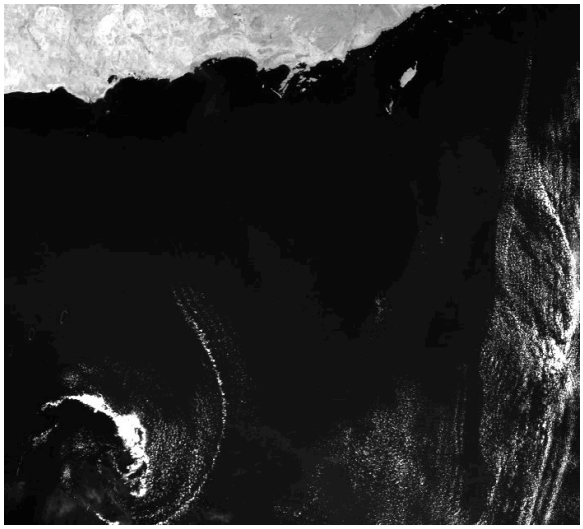

Band 2 (0.87 micron)

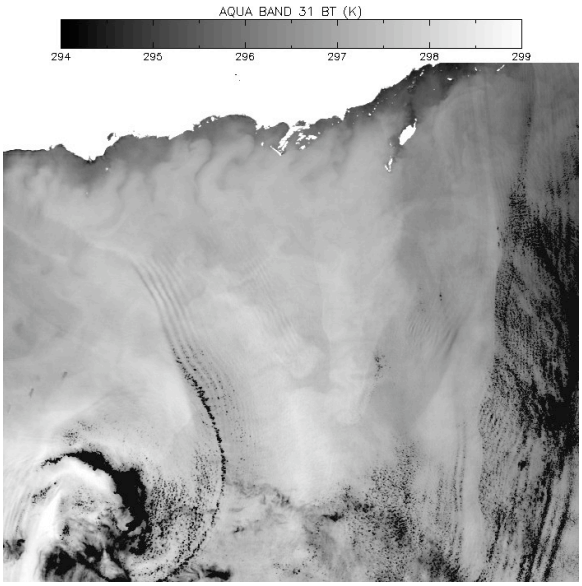

Band 31 (11.0 micron)

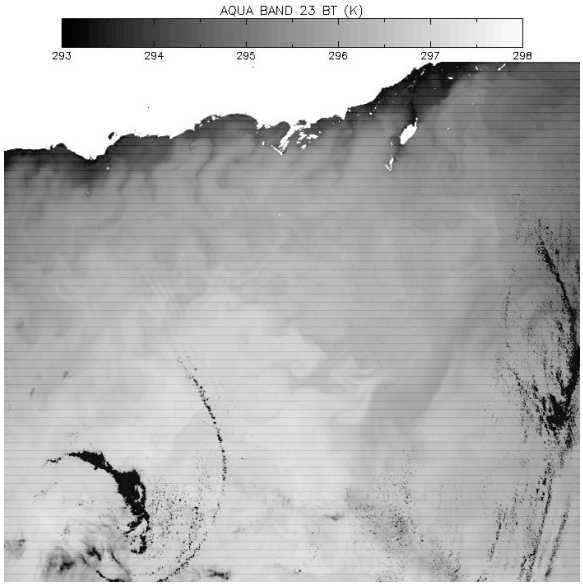

Band 23 (4.05 micron) original

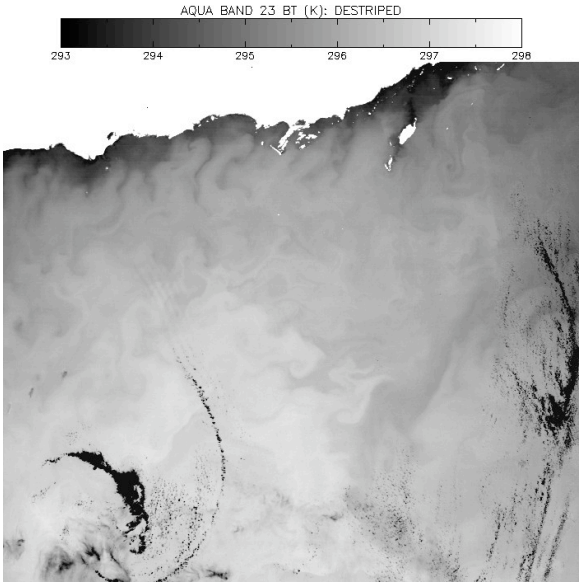

Band 23 (4.05 micron) destriped

Figure LG2. Example of Aqua MODIS Destriping
MYD021KM.A2003147.0555.003.2003149154542.hdf (2003/05/27, 05:55 UTC)
Northwest Shelf of Western Australia, 700 x 700 pixel subscene

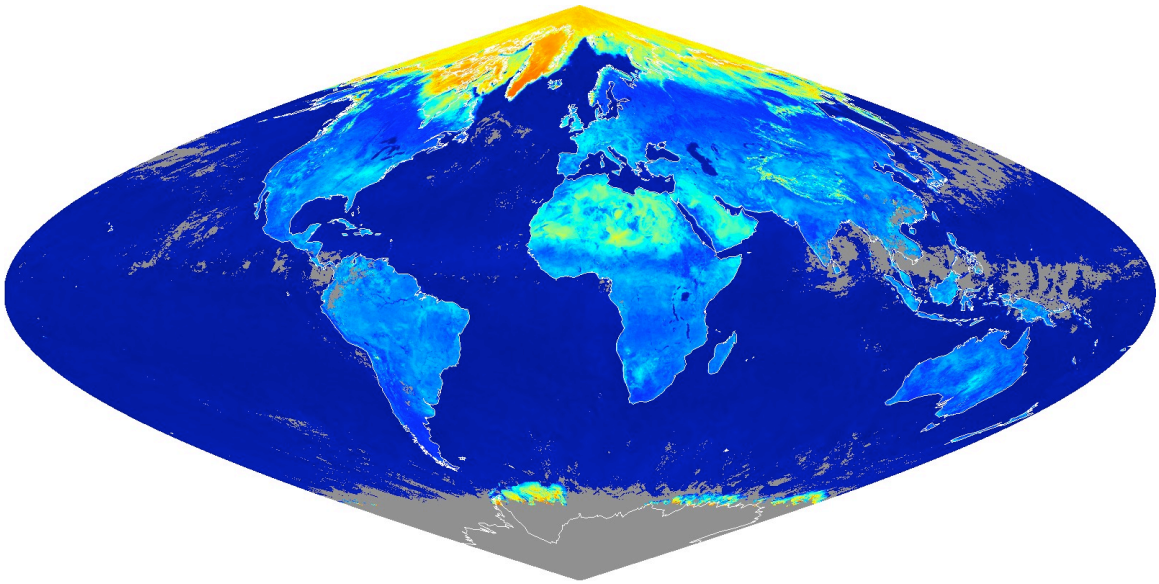

Figure LG3. Terra MODIS band 2 (0.87 μm) clear-sky reflectance composite for 2003/05/11-18

Clear Sky Radiance Investigations

A thorough investigation into the production and use of the clear sky radiance MODIS products has begun by Richard Frey and Kathy Strabala. Problems arose with the original daily and eight-day compositing software after the decision to move to 27 bands instead of the original 8 caused the software to exceed the memory limits on the UW software development machine. The re-engineering that was required to fix this provided the UW with the opportunity to re-evaluate the requirements and use of the clear radiance files.

A series of meetings has been held to define the exact clear radiance requirements, inputs and outputs. The requirements are based upon the use of the files for:

1) Detection of cloud shadows. Comparison between observed clear sky and the clear radiance bands 2, 6 and 7.
2) MOD35 temporal consistency checks. Comparison of the 8 day clear sky radiance files to current observations in bands 2 and 31.
3) MOD06CT bias correction. A correction between the observed clear and calculated clear based upon a forward calculation. The input biases will be computed in a rolling eight day window of daily clear radiance file composites for bands 31, 33-36.
4) MOD07 bias correction. A correction to the input channels using a clear minus calculated clear value determined from forward model calculations. The biases will be used as input and updated monthly or seasonally for bands 24, 25, 27-36.

Many factors affect the quality of the clear sky radiance product. These include the confidence level chosen as the cloud mask clear threshold (>.95% or > .99%), the viewing zenith angle of the clear sky observation, the detectors used in the compositing, whether or not sunglint regions are included, etc. Bias correction quality is also dependent upon the accuracy of the forward model you choose. A thorough examination of these issues is necessary before the optimal

criteria for a pixel to be included in the clear sky radiance composites can be determined. As a means to this end, test software, which allows a user to manually select clear sky criterion is being written. The test software must be able to:

1) Process a given clear confidence level threshold (> .95%, > .99%, etc.)
2) Process one or more detectors selected by the user (1-10).
3) Process a bin of viewing zenith angles (ie., $0 < \theta < 30$).
4) Process with or without sunglint regions included.
5) Process with or without nearest neighbor checks.
6) Process one or more bands selected by the user.
7) Include forward calculation (for longwave IR bands)
8) Must be configurable - able to include or exclude the cloud mask bits selected by the user. For instance, you may not want to include scenes where the cloud mask thin cirrus bit indicates cloud.

Output file contents were determined based upon the end user requirements:

1) Grid cells at 25 km resolution
2) Separate Night and Day statistics
3) Visible bands will be stored in MODIS reflectance units
4) Infrared bands will be stored in MODIS radiance units

These statistics will be store for each band and each grid cell:
1) Total number of observations.
2) Number of clear observations.
3) Number of land pixels.
4) Number of water pixels.
5) Sum of observations of clear radiances/reflectances.
6) Sum of the square of observed clear radiances/reflectances (for calculation of variance.)
7) Sum of viewing zenith angles.
8) Sum of observed minus calculated radiances for each infrared band.
9) Sum of the square of the observed minus calculated clear radiances for each infrared band (for calculation of the variance)
10) Maximum value.
11) Minimum value.

From these stored parameters, it will be possible to calculate the average, standard deviation and variance for each band and each daily and eight day 25 km grid cell observation and bias. It is expected that the test software will first be applied and automated to work with UW direct broadcast data. Comparisons between different clear pixel criteria will be made and the final choice of input parameters will be determined and then tested on global data.

The second piece of the clear radiance file effort has been in the selection of the best forward model to use for the determination of the bias. UW has historically used the PLOD (Pressure Layer Optical Depth) fast model transmittances based upon MODIS spectral response functions. However, problems may be present in the duplication of the statistics (dependent set) when

compared with the original LBLRTM transmittances in the versions currently in use in our production software (version 6.01). In addition, it was found that there was an error in the MODIS spectral response function files that were used to generate the transmittances. This problem was minor but brought to light our need to know more about the generation and use of the fast model as part of the UW operational products.

In light of these issues, UW has begun an investigation aimed at identifying the best forward model to use in our operational products and for the generation of the clear sky radiance files. This effort includes examining all inputs to the model. Global numerical model profiles, ozone profiles and surface skin temperature, pressure and emissivity are being evaluated for their effects on the performance of the forward model. The final determination of a model and inputs will be based upon a comparison of statistics, ease of use as part of our production software (efficiency), advice from modeling experts at UW, and finally the effect on products MOD06 and MOD07. Final analysis is expected to take place in 3rd quarter 2003. The goal will be to have the clear radiance file processing in place, and the bias corrections in use before the start of MODIS Terra reprocessing with collection 5.

MODIS Clear Radiance Data Set for NWP Assimilation Tests

A clear-sky radiance dataset was provided by Julie Whitcomb and Liam Gumley to the European Center for Medium Range Weather Forecasting (ECMWF). The data was obtained from Terra MODIS during the period March 1, 2001 (day 60) to March 31, 2001 (day 90). The MODIS clear-sky products (MODCSR_G) from Collection 4 for each granule in this time period (a total of 8825 granules) were analyzed to extract TOA reflectance for bands 1-7, 17, 18, 19, and 26, and TOA radiance for bands 20-36. No atmospheric correction or view angle correction has been performed. The results were composited onto a global sinusoidal equal area grid with cell dimensions 25 x 25 kilometers (total of 814880 grid cells).

Clear-sky parameters stored for each band for each grid cell include (1) Number of observations, (2) Sum of observations, (3) Minimum observation, and (4) Maximum observation. Day and night observations are treated separately; day observations are those where the MODIS instrument is in day mode and the local solar zenith angle is less than 85 degrees and all other observations are night. Any pixel at 1 km resolution identified by the MODIS cloud mask as Probably Clear or Confident Clear is classified as a clear-sky observation. Supporting source code to unpack the gridded data, along with global images for each day, were supplied along with the analyzed data, which added up to about 750 MB per day.

MODIS Cloud Mask (MOD35) Modifications

Algorithm adjustments were studied by Richard Frey and Steve Ackerman to improve snow detection, smoke detection, and nighttime cloud detection.

Snow Detection
An adjustment was made to the Aqua snow detection algorithm. Previously, band 7 (2.1 μm) reflectances were substituted for those of band 6 (1.6 μm) due to the poor quality of the latter. During the winter (2002-2003) months, it became obvious that a band 7 threshold set during the

autumn of 2002 was not adequate for winter conditions in the far north. Many clear-sky, snow-covered scenes were being falsely identified as cloudy. The band 7 reflectance threshold was changed from 0.050 to 0.095. Note that the Normalized Difference Snow Index (NDSI) threshold for Aqua data remains unchanged at 0.75.

In addition to the NDSI test, several reflectance and brightness temperature checks are made in order to reduce the number of false positive snow identifications. The band 7 reflectance test mentioned above is one of these. Another such test is performed using an 8.5-11 μm BTD (≥ 0.5 is cloud). It is designed to help discriminate between ice clouds and ice at the surface of the earth. A refinement was added, where we also require that the 3.75-11 μm BTD is ≥ 9K. In very cold and dry atmospheres, 8.5-11 μm BTDs sometimes satisfy the above cloud threshold even under clear sky conditions.

Smoke Detection

The MOD35 smoke detection algorithm has been modified and tested but not yet included in the operational code. Two reflectance ratio tests have been added to the previous requirements. For smoke to be identified:

band 3 (0.47 μm) / band 1 (0.65 μm) ≥ 0.85, and

band 2 (0.86 μm) / band 1 (0.65 μm) ≥ 1.0.

Also, the standard deviation of band 1 reflectances over a 3x3 group of pixels (pixel of interest in the center) must be ≤ 0.04. These changes greatly reduce the number of cloudy pixels misidentified as smoke. Figure RF1 shows an example from 6 July 2002

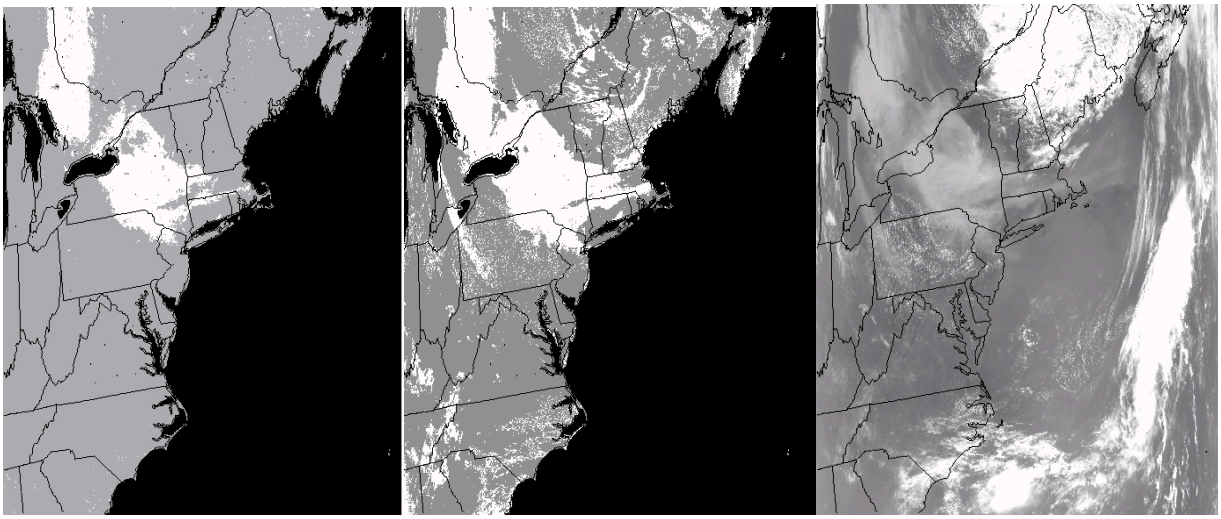

Figure RF1. Terra MODIS Band 3 image (right), previous (center) and proposed (left) "smoke mask" for July 6, 2002 at 15:50 UTC.

Cloud Detection Comparisons

An effective method of assessing cloud detection algorithms is to compare associated clear-sky radiance data. Terra MODIS clear-sky reflectances and brightness temperatures (resulting from application of MOD35 to Level 1b radiances) were compared to those of NOAA-16 AVHRR taken from the CLAVR method. Figure RF2 shows monthly mean July 2002 MODIS and

CLAVR clear-sky 0.65 μm reflectances. The two maps are very similar; however, the MODIS data show greater discrimination between ice and clouds near the terminator in the southern ocean near Antarctica.

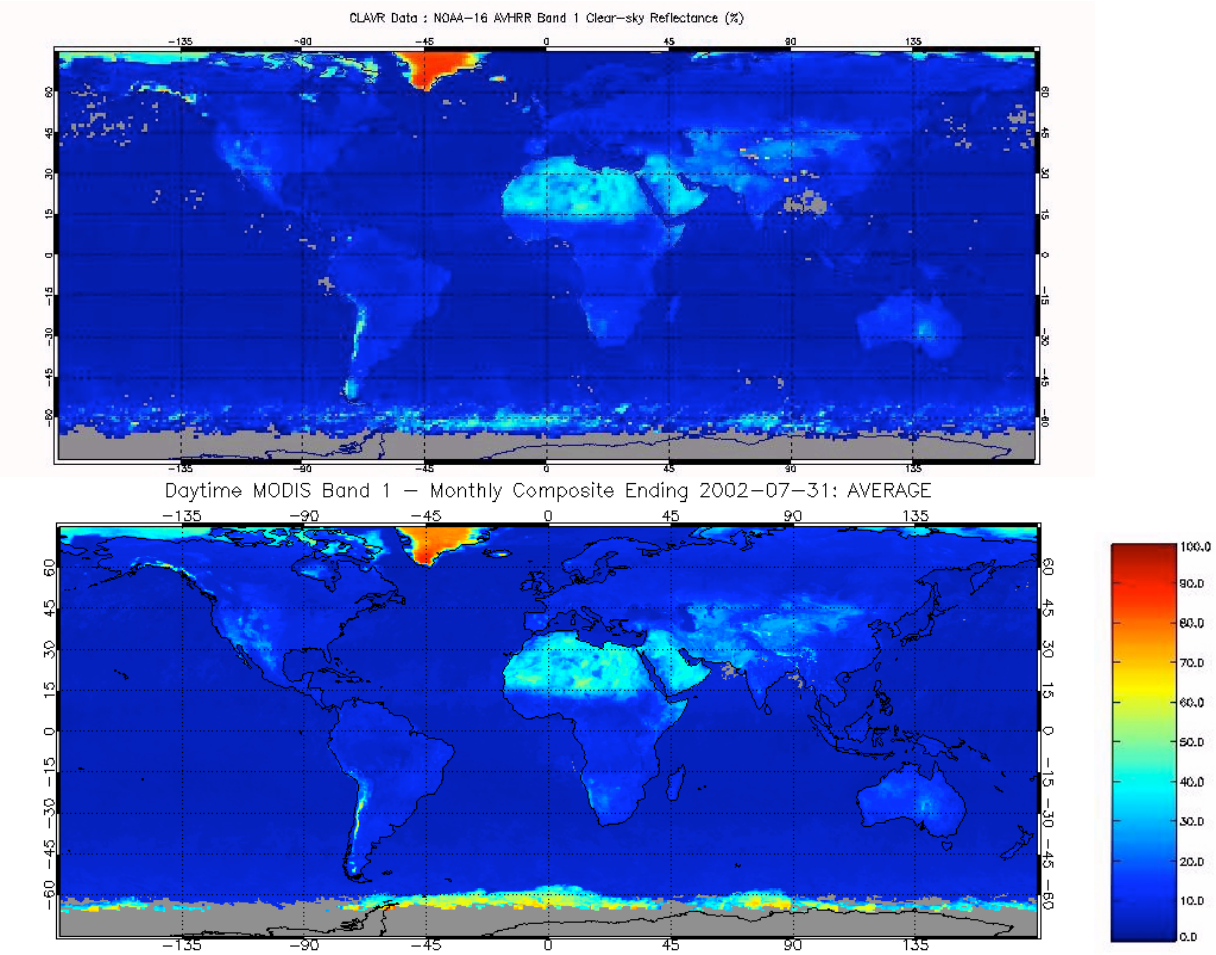

Figure RF2. NOAA-16 AVHRR (top) and Terra MODIS (bottom) 0.65 μm monthly mean clear-sky reflectances from July 2002.

UW compared MODIS cloud mask results with ground-based Micropulse Lidar/ Millimeter Cloud Radar (MPL/MMCR) cloud top height data from the SGP CART (Southern Great Plains Cloud and Radiation Testbed) site in Lamont, OK. The data were taken at daytime Terra overpass times beginning in October 2000 and extending until March 2002. There are inherent difficulties in comparing data with vastly different spatial and temporal resolutions and sensitivities. Since the MPL/MMCR is subject to attenuation effects and local cloud height deviations at any single observation point, the data was compiled in the following way. Each MPL/MMCR retrieval within +/- five minutes of the MODIS observation time was placed into one of several 500-meter range bins. Range bins were valid (indicated useful cloud height estimates for comparison) if they accounted for at least 40% of the data points in a MPL/MMCR measurement period (10 seconds). These values were then averaged over the 10-minute period and compared directly to MODIS cloud mask results (single pixel closest to SGP site). The results of the comparison are shown in Table RF1. The MODIS cloud mask algorithm and

MPL/MMCR agreed on the existence of clear or probably clear 86% of the time (86+65/175) and 92% of the time that a cloud was present. An uncertain result occurred in less than 3% of the total comparisons.

Table RF1. MPL/MMCR lidar/radar and MODIS cloud mask (MOD35) cloud frequency comparison.

Radar/lidar	MODIS Cloud	MODIS Uncertain	MODIS Probably Clear	MODIS Clear	
Clear	19	6	85	65	175
Low Cloud	82	0	4	3	89
Middle Cloud	44	3	13	0	60
High Cloud	14	1	6	3	24
	159	10	108	71	

Effects of Field of View Size and Sampling Strategies Using MODIS 1-km Data

A study of the effects on clear-sky detection and clear vs. cloudy radiance data at various field of view (FOV) sizes and sampling frequencies is underway. MODIS cloud mask and 1-km radiance information are being used to simulate measurements and/or sampling strategies from instruments with various footprint sizes. One question to be considered is how MODIS clear-sky data might be utilized as input to atmospheric temperature and moisture profile retrieval algorithms that use sounder data from instruments with larger FOVs. For example, how many 1-km clear-sky MODIS pixels are required in order to adequately specify the clear radiances within an AIRS (Atmospheric Infrared Sounder) or AMSU (Advanced Microwave Sounding Unit) footprint? How quickly does the probability of finding clear pixels decrease with increasing FOV size?

Figure RF3 shows the probabilities of sampling clear skies in daytime ocean scenes as calculated for Terra data on August 24, 2002 for various sub-sampling (FOV) sizes located within an AMSU footprint (about 48-km resolution). The x-axis shows FOV size and the various curves represent how many clear sub-samples one requires. The resulting probabilities are shown on the left-hand side and overall cloud amounts on the right-hand side (asterisks). Even with average cloud amounts of about 70%, there is still about a 0.7 chance of finding at least 1 clear-sky 1-km pixel within any given AMSU FOV. That probability drops to about 0.25 for 10-km sub-samples, and to about 0.1 if one requires at least 8 of these (about half of the total area of an AMSU FOV). Notice also that the slopes of these lines change at a sub-sample size of 10 km.

Figure RF4 shows average cloud forcing for the same scenes. In this plot, the x-axis lists the minimum number of required clear-sky sub-samples within an AMSU footprint and the curves represent sub-sample sizes (1 km to 16 km). One can see that FOV (or sub-sample) size has a large effect on cloud forcing values. Presumably, as one moves to larger FOVs, more and more clear spots ("holes" in the clouds) are present in the "cloudy" (not clear) sub-samples, leading to lesser amounts of cloud forcing. The cloud forcing results for the largest sub-sample sizes are also biased towards warmer regions since daytime partly cloudy AMSU footprints having at least one large, clear-sky sub-sample are generally characterized by lesser cloud amounts and warmer temperatures (plot not shown).

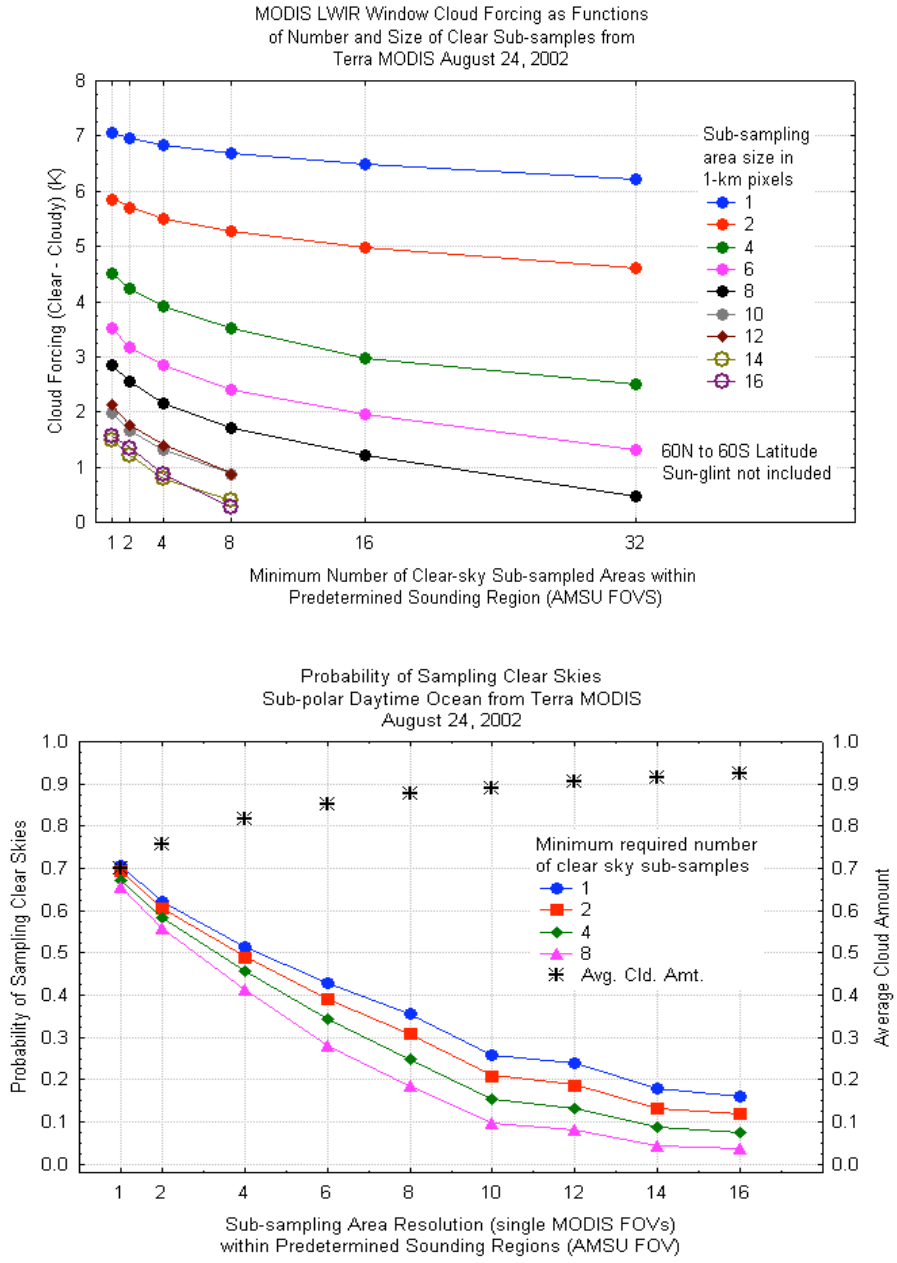

Figures RF3 (top) and RF4 (bottom). See text for explanations.

Cloud Masking in Polar Regions

Validation of the MODIS cloud mask has been done by Jeff Key and Yinghui Liu using surface-based radar and lidar observations at two locations in the Arctic and one location in the Antarctic. At Barrow and Atqasuk (the North Slope of Alaska/Adjacent Arctic site) and South Pole, a cloud mask derived from millimeter-wavelength cloud radar (MMCR), a Vaisala ceilometer (VCEIL) and a micropulse lidar (MPL) was compared with the collocated MODIS cloud mask product in both daytime and nighttime from January 2001 to December 2002. In the

daytime Arctic, about 7% of the cloud identified by radar/lidar is identified as clear by the MODIS cloud mask, and about 7% of the clear identified by radar/lidar is identified as cloud by the MODIS cloud mask. Considering temporal and spatial differences between radar/lidar and MODIS observations, the MODIS cloud mask in polar regions in daytime is acceptable.

In the nighttime Arctic, about 49% of the cloud identified by radar/lidar is identified as clear by the MODIS cloud mask, and about 6% of the clear identified by radar/lidar is identified as cloud by the MODIS cloud mask. In nighttime Antarctic, about 20% of the cloud identified by radar/lidar is identified as clear by the MODIS cloud mask, and 0% of the clear identified by radar/lidar is identified as cloud by the MODIS cloud mask. This reveals a significant deficiency in the MODIS cloud mask during the polar night, where much of the cloud is not detected.

Some existing cloud and clear tests have been modified, and additional tests have been formulated. The 3.9-12 μm BTD test has been modified to account for its dependence on temperature. Three new tests for the Arctic and two new tests for the Antarctic have been added, including a 11-7.2μm brightness temperature difference test for low cloud in the Arctic, a 11-12μm brightness temperature difference test for high cloud, a 14.2-11μm brightness temperature difference test for the Antarctic, and a 7.2-11μm test for low-level temperature inversions in the Arctic. With these modifications and new tests, significant improvement can be seen. In the Arctic at night, about 17% of the cloud identified by radar/lidar is now identified as clear by the MODIS cloud mask, and about 6% of the clear identified by radar/lidar is identified as cloud by the MODIS cloud mask. In the Antarctic at night, about 3% of the cloud identified by radar/lidar is identified as clear by the MODIS cloud mask, and about 4% of the clear identified by radar/lidar is identified as cloud by the MODIS cloud mask. The comparison is shown in the table below.

Table JK1: Comparison of radar/lidar and MODIS cloud detection in polar night conditions.

			Arctic Night		Antarctic at Night	
	Radar/ Lidar	MODIS	# of cases before change	# of cases after change	# of cases before change	# of cases after change
1	cloud	cloud	332	541	331	439
2	cloud	uncertain	8	33	31	2
3	cloud	probably	47	2	9	0
4	cloud	confident	328	116	82	12
5	clear	confident	211	216	217	208
6	clear	probably	23	3	0	0
7	clear	uncertain	7	12	0	1
8	clear	cloud	15	16	0	8

MODIS Cloud Top Properties (MOD06)

In response to a request from a MODIS data user, cloud top temperatures as low as 190K are now accumulated and reported by the MODIS Atmosphere Level 3 algorithm. It was pointed out that some of the deepest tropical convective clouds may reach temperatures this low. The previous lower limit was 220K.

Figure RF5 shows a comparison between MODIS and ISCCP high cloud frequency for the month of December. MODIS data is from December 2002, while ISCCP is the mean of all Decembers from 1983-2001. High clouds are those with cloud top pressures < 440 mb and latitudes are 75S to 75N. The patterns are similar between the two data sets but MODIS displays sharper contrasts between regional climates (for example, between subtropics and the ITCZ), though time averaging in the ISCCP data has undoubtedly lessened contrasts.

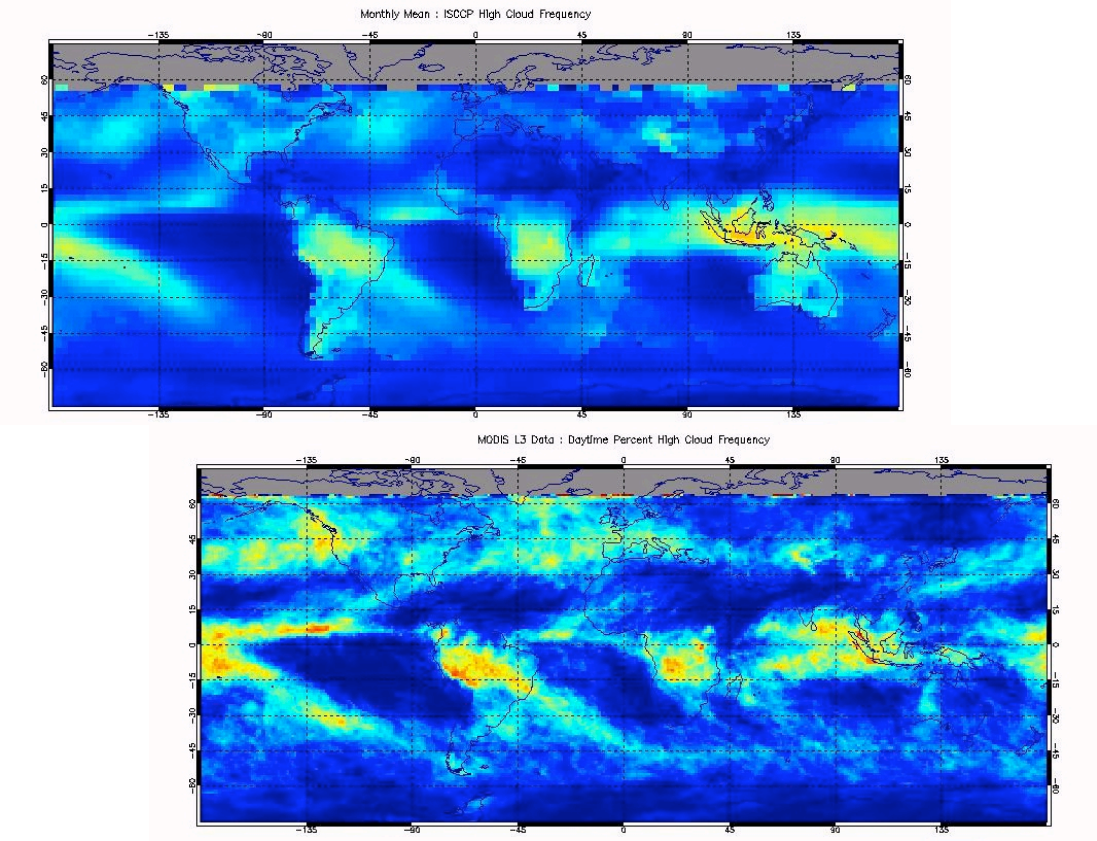

Figure RF5. Comparison of MODIS (December 2002) and ISCCP (Decembers from 1983-2001) high cloud frequency.

Figure RF6 shows a comparison between Terra and Aqua high cloud frequencies on 24 August 2002. As expected, Aqua data shows a higher frequency than Terra over land surfaces during the daytime due to more solar heating, while ocean data is more similar.

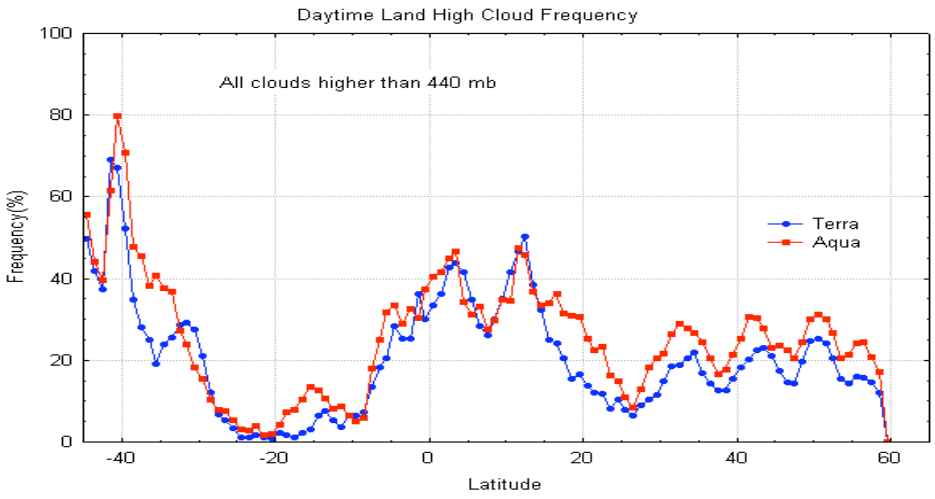

Figure RF6. Comparison of Terra and Aqua high cloud frequencies on 24 August 2002.

Validation of MODIS Cloud Top Pressures Using MISR

Catherine Naud from the University College in London, England visited the UW MODIS team from mid April through mid-May. She was able to
1. Compare MISR CTH with MODIS and MERIS CTP for 14 Jan 2003, 20 Jan 2003 and 15 Feb 2003 over the SGP site.
2. Compare MISR and MODIS 1km CTH over Texas on 27 Nov 2002 during the Texas-2002 ER-2 campaign.
3. Prepare a list of coincident MISR, MODIS and radar measurements over SGP site for 2001 (2000 and 2002 to follow), and over Chilbolton for 2000-2001 and communicated these for a next set of comparisons.

The outcome of these comparisons was interesting. For the 2 SGP cases with high thin clouds (14 Jan 2003 and 30 Jan 2003), MODIS CTP tend to be too high at thin cloud edges until optical depth so small that CTP refers to low clouds. The impact of surface temperature on MODIS CTP retrieval was tested but was not identified as the primary cause of this problem. Further tests are to be performed at SSEC using these cases. In both cases MERIS did not detect these high clouds over the SGP, strong winds were present and we suspect that these high clouds moved towards the SGP site between ENVISAT and Terra overpasses (30 minutes difference). MISR CTHs behave better at cloud edge but seem to be distributed randomly between 0 and 15km, which indicates that it also has a problem with thin high clouds although probably not at cloud edge. For the SGP case with low clouds, good agreement was found between radar, MERIS and MISR CTH. MODIS CTH too low. For the Texas cases: very good agreement between MODIS CTH (1km) and lidar, problem with MISR: lots of undetected clouds and heights too low. Possibility of overlap in area where Terra and ER-2 overpass: to be tested. Also other stereo matchers tested for MISR, still need to get good CTH from matcher output.

Possible future work will include systematic comparison over SGP, NSA and TWP for ARM sites, and Chilbolton in UK. When enough cases are gathered the cloud conditions must classified and the performance of instruments categorized.

Multi-layered Cloud Detection

Rapid progress has been made on the automated detection of multi-layered clouds in daytime MODIS data due to the efforts of a particularly adept CIMSS/MODIS graduate student, Greg McGarragh, advised by Bryan Baum. The detection process is now being applied to both Terra and Aqua data collected in near real-time with the direct broadcast system at CIMSS. As the software for this detection process is fully in C, rather than the former Matlab software, a full granule is processed in approximately 30 seconds on a desktop linux workstation. A set of web pages describing this effort is now available at http://cimss.ssec.wisc.edu/multilayer.

The IR-based cloud thermodynamic phase product is generated at 5-km resolution in the operational environment. However, as part of the multi-layered cloud detection process, the cloud phase is being generated at 1-km resolution. An example is provided in Figure BB1. This Terra scene, recorded 1 July 2003 at 1458 UTC, contains a high-level ice cloud deck that overlies a low-level water deck in numerous places. One important item to note is that the IR cloud phase product has no evidence of striping at 1-km resolution; the new destriping algorithm has had a very beneficial effect here.

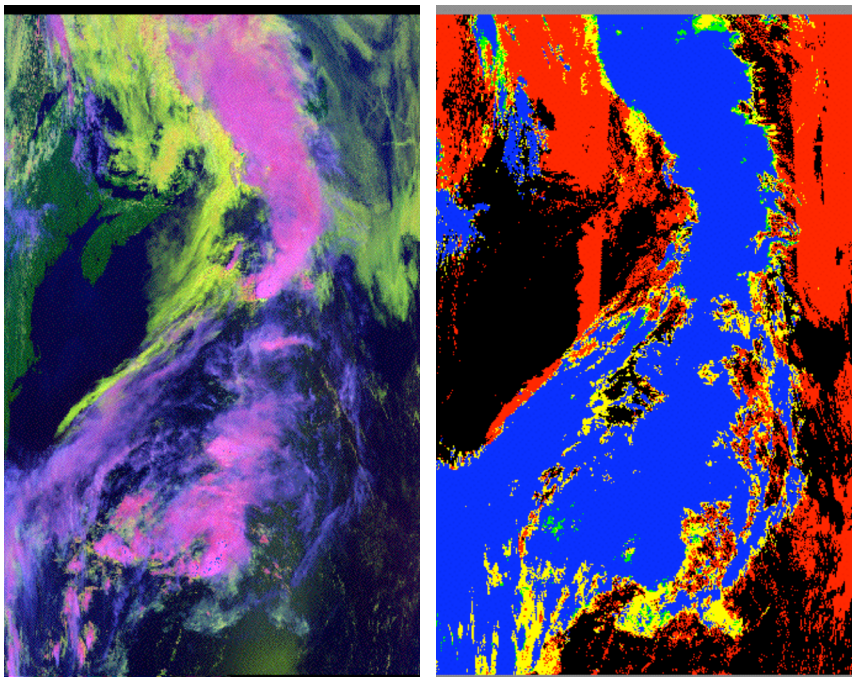

Figure BB1: In the left panel is a false color image created from a combination of MODIS bands 1, 6, and 31 (R: band 1, G: band 6, and B: band 31, flipped). High ice clouds are pink or blue, low water-phase clouds are yellow, land is green, and water is dark blue. In the right panel is the R-based cloud phase, with ice clouds (blue), water clouds (red), mixed phase clouds (green), and uncertain phase (yellow).

Given the cloud clearing and cloud phase products at 1-km resolution, the multilayered cloud detection method is applied to the granule, with results shown below.

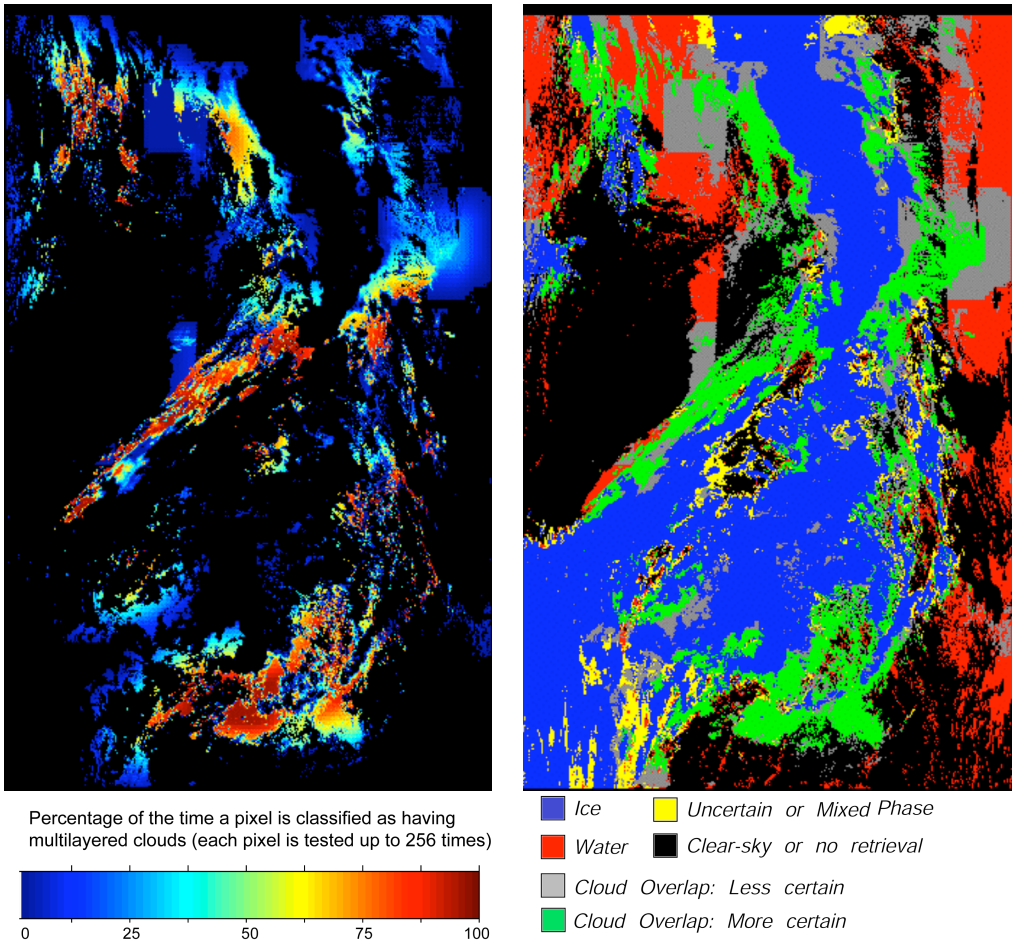

Figure BB2: The left panel denotes the results from the multilayered cloud detection effort, with the red color denoting the pixels having the highest potential for being multilayered. The right panel merges the cloud phase and multilayered cloud results into a single product (suggested by Dr. Catherine Naud during her visit to CIMSS).

Visual comparison of the multilayered cloud product with the false color image shown above indicates that our approach has some facility for detecting when optically thin ice clouds overlie a low-level water cloud. Efforts are ongoing to validate the approach more extensively. The MODIS DB site is a necessary and useful testbed for continuous testing of the approach, and we are becoming more enthusiastic for transferring this method into the operational environment in the near future. These data products are available for each daytime Terra and Aqua overpass for 8 days, with new overpass products replacing the earliest ones.

Atmospheric Profiles

A new version of the operational MOD07 product code was prepared by Suzanne Seemann and delivered to SDST on 2 June 2003. In the prior algorithm, MODIS MOD07 retrievals had some

errors related to radiance bias corrections, including a discontinuity in retrievals at latitude 50N, and a dry bias in TPW retrievals for moist cases. Retrievals were also noisy, particularly on Terra due to striping among detectors. This noise was enhanced by our use of the difference between two bands (25-24) as a predictor. Retrievals over extremely warm surfaces (daytime Sahara in August) showed noise due to instability of the algorithm. Updates to the algorithm are summarized below and examples of improvement are also provided.

1) In the new algorithm radiance bias corrections were improved and now can be a function of GDAS TPW or MODIS brightness temperature, as opposed to latitude. This avoids sharp discontinuities along latitude lines and allows us to better characterize the bias corrections. Bias values also are now read in from a separate file instead of hardwired into the code.
2) In order to reduce noise due to striping, certain detectors were flagged as noisy or out of family and these are now skipped in the retrieval. We further reduced noise by removing the regression predictor based on the difference between the BT of bands 25 and 24. Instead of this difference, only BT 25 is now used. This is possible without affecting desert retrievals because of improved emissivity characterization in the desert areas.
3) New emissivity values with a more physical basis were assigned to the training data profiles, improving retrievals over very hot scenes. With the new emissivity, noise in very hot desert areas due to unstable retrievals does not occur anymore. More information on this is provided in the section on training data.
4) The latest version of the PFAAST forward model for MODIS based on calculations using the HITRAN2000 spectral data base was included in the coefficient calculations.
5) Retrieved skin temperature is now written to the Surface_Temperature product SDS. Previously, only a copy of NCEP-GDAS surface temperature was written to this field.
6) Improved handling of the surface level was incorporated into the TPW integration.

With this new algorithm, Terra MODIS TPW comparisons with microwave radiometer at the SGP CART site for 80 cases over 1.5 years improved from 4.5mm RMSE to 3.1mm (See Figure SWS1). The most significant differences exist for moist cases. Previously, MODIS was on average too dry for the cases with TPW > 20mm; now there is still some scatter but no clear bias. Additionally, the moist bias for dry cases has been reduced, but not completely overcome, in the new algorithm. Figure SWS2 compares TPW retrieved with the old and new MOD07 algorithm with GOES for a moist and a dry case. Aqua MODIS TPW compares better with GOES with the new algorithm, as shown for one case in Figure SWS3.

Training Data
Improvements to the current NOAA88 training data base are being studied. Work this period with the training data includes testing a combined NOAA88/TIGR-3 data base of profiles and studying improvements to the surface characterization of the profiles in these data bases. Improved surface emissivity characterization was implemented as part of the recent delivery and is summarized here. In addition, physical relationships between surface air temperature and skin temperature are being investigated for use in future training data sets.

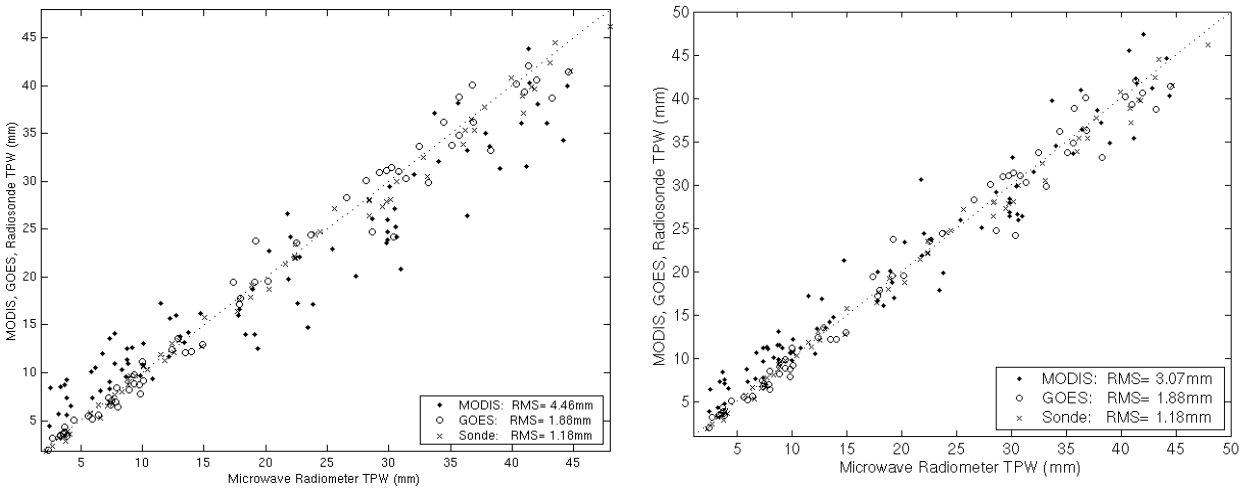

Figure SWS1. Comparison of Terra MODIS TPW at the SGP CART site with GOES TPW, radiosonde TPW, and microwave radiometer TPW for 80 cases from April 2001 to August 2002. All cases in the left-hand comparison were processed with the operational algorithm running for collection 4. The latest algorithm just delivered in June 2003 was used to reprocess all cases for the comparison on the right

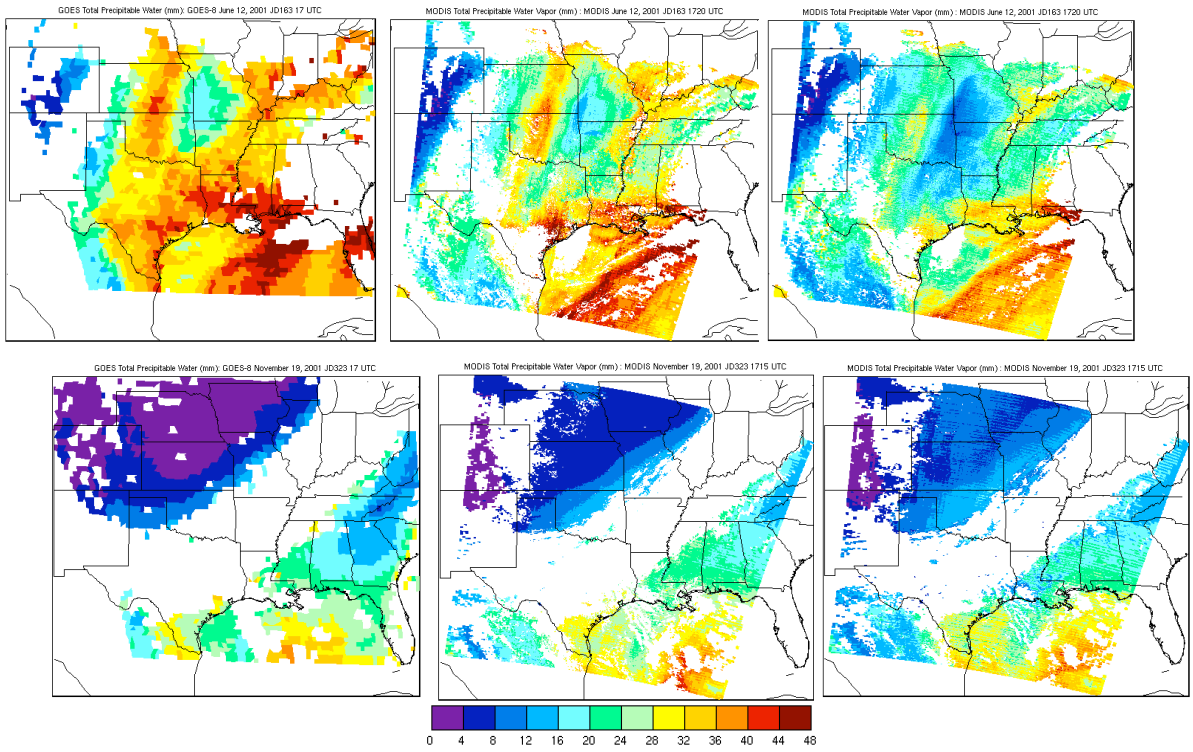

Figure SWS2. TPW (mm) from GOES-8 (left), Terra MODIS processed with the new algorithm (center), and from Terra MODIS with the old, collection 4 algorithm (right) for two cases: June 12, 2001 1730 UTC (top row) and November 19, 2001 1715 UTC.

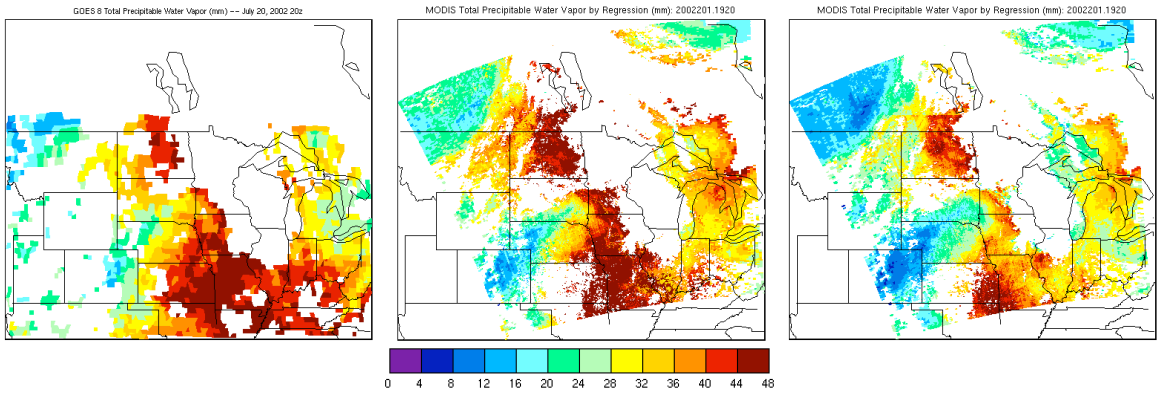

Figure SWS3. TPW (mm) from GOES-8 (left), Aqua MODIS processed with the new algorithm (center), and from Aqua MODIS with the old, collection 4 algorithm (right) for July 20, 2003 at 1920 UTC.

Surface Emissivity

The emissivity assigned to the training data profiles in the version of NOAA88 currently used as training data for the MOD07 algorithm has a mean of 0.85 at 4 m, and 0.95 between 9 m and 14 m, with a linear interpolation in between (see Figure SWS4a). A standard deviation was applied to these values to simulate some variability. This approach did not properly represent actual emissivities, particularly in desert regions. Removing most of the emissivity signal by differencing MODIS bands 24 and 25 in the collection 4 algorithm made significant improvements in retrievals over the desert. However, during extremely hot conditions such as those found in the Sahara desert in August, some problems still existed. TPW from Aqua MODIS in Figure SWS4b shows along-track stripes of high moisture due to unstable retrievals on this hot day in August 2002. To address this problem, more representative emissivity values were assigned to each of the training profiles. Each profile were categorized as ocean, snow/ice, desert, and non-desert land, and an approximate emissivity was derived for each based on measurements by Zhengming Wan and the UCSB MODIS land surface temperature group (http://www.icess.ucsb.edu/modis/EMIS/html/em.html). The new emissivities used for the desert profiles are shown in Figure SWS4c, and the improvement in the TPW retrievals using the training data set with the new emissivity is in Figure SWS4d.

Skin Temperature

In order to assign a more physically realistic skin temperature to the training profiles, measurements of skin temperature collocated with radiosondes are being collected over a variety of ecosystems for different times of year. This data will enable us to develop physically-based relationships between measured lowest level radiosonde air temperature and skin temperature. These relationships will be used to assign a skin temperature to the training profiles. Sites that we are collecting data from that regularly make measurements of skin temperature (infrared thermometer) and launch radiosondes include the ARM CARTs in Oklahoma, Alaska, and the Tropical Western Pacific. In addition, data from the Marine AERI such as the one on the "Explorer of the Seas" in the Caribbean and the Polar AERI such as those at the South Pole and Dome Concordia will be used.

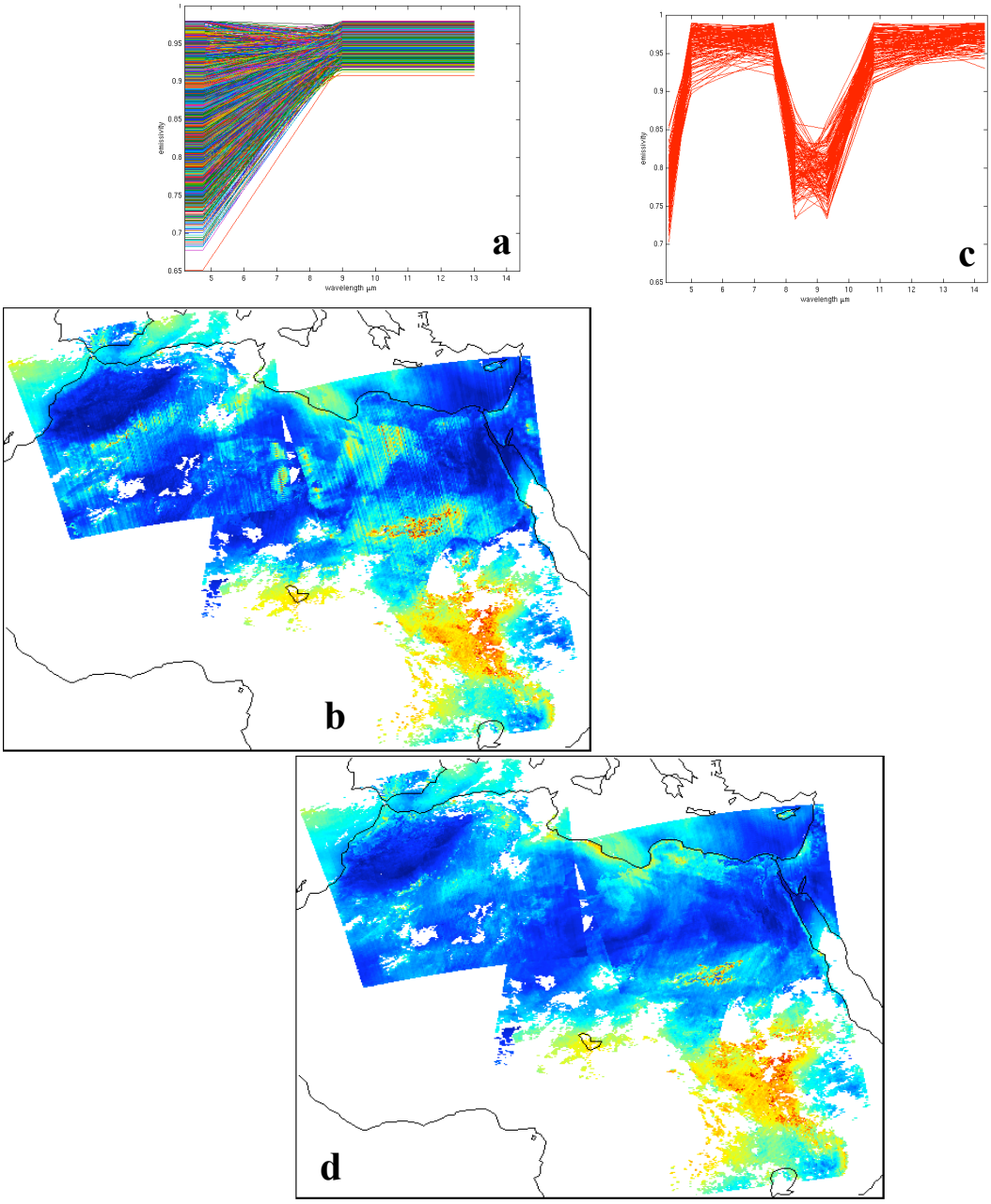

Figure SWS4. a) Emissivity spectra for all training data profiles used in the original algorithm. b) Aqua MODIS TPW (mm) for August 24, 2002 over the Sahara desert retrieved with coefficients derived using the emissivity spectra in (a). c) New emissivity spectra for desert profiles. d) As in (b) except retrieved with coefficients derived using different emissivity spectra for ocean, ice and snow, desert, and non-desert land such as those for desert shown in (c).

Preliminary relationships between skin temperatures and surface air temperatures have been derived from measurements at the SGP CART site in Oklahoma. Figure SWS5a shows this relationship for 131 cases over two years. There is a consistent day/night difference in the skin temperature/surface air temperature (ST/SAT) relationship, indicating that any relationship must be a function of solar zenith angle. UW fit a line to the ST/SAT *difference* for both day and

night to come up with a slope, y-intercept, and standard deviation to characterize the relationship. The result of applying this relationship, plus a simple approximation of the ST/SAT for ocean (based loosely on MAERI measurements), to the combined NOAA88/TIGR-3 data base is shown in Figure SWS5b. These training data bases with the new skin temperatures were used to create regression coefficients for the MOD07 retrieval. Results (not shown) are encouraging, however ST/SAT relationships over a wider range of ecosystems (particularly deserts) are needed to properly characterize all the conditions viewed by MODIS.

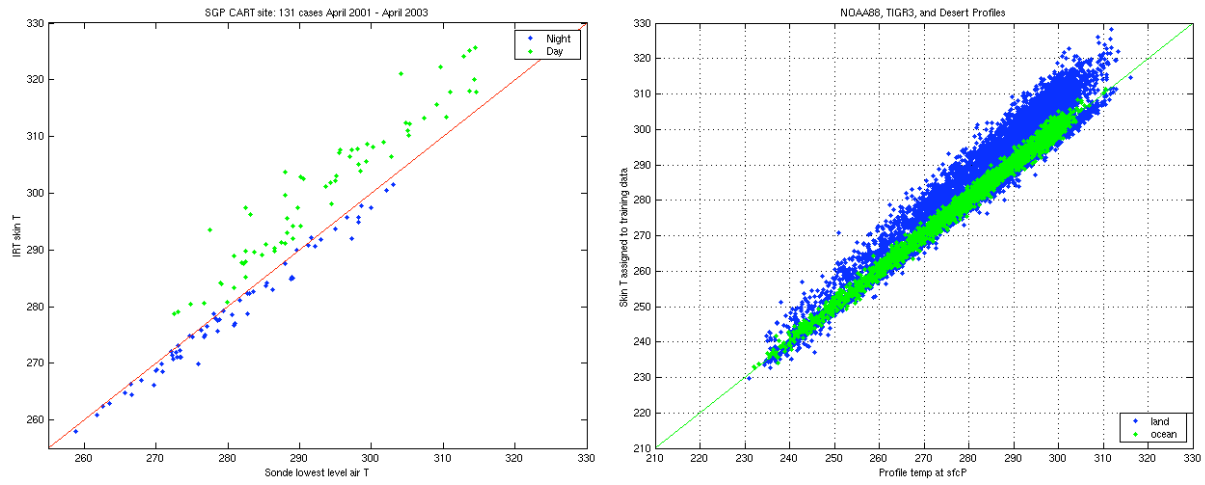

Figure SWS5. Left: SGP CART site IRT measurements of skin temperature as a function of radiosonde lowest level air temperature for 131 cases over two years (April 2001 to April 2003). Green dots correspond to daytime cases, blue to nighttime. The red line represents conditions where skin temperature is equal to surface air temperature. Right: skin temperature vs. the surface air temperature for the combined NOAA88/TIGR-3 profile database after applying the relationships derived from measurements shown at the Left over land, and a simple relationship for ocean.

Radiance Bias

Observed minus calculated radiance bias values continue to be explored. Biases for all MODIS bands, separately for all 10 detectors were calculated for a few global days. Global averages, as well as global maps of bias, and global relationships between bias and TPW or bias and BT were derived. One example of a global map of bias for Band 33, detector 3 is shown in Figure SWS6. For this day, only clear sky ocean scenes with zenith angle < 20 degrees were included. Input to the forward model for skin temperature was Reynolds blended SST, and tests were made with both ECMWF and GDAS profiles as input. Bias calculations based on direct broadcast data received at CIMSS have also been implemented and can be run for any Aqua or Terra overpasses day or night. This provides a useful tool for testing inputs to the bias calculation because different skin temperature, emissivity, or profile data can be substituted for comparison.

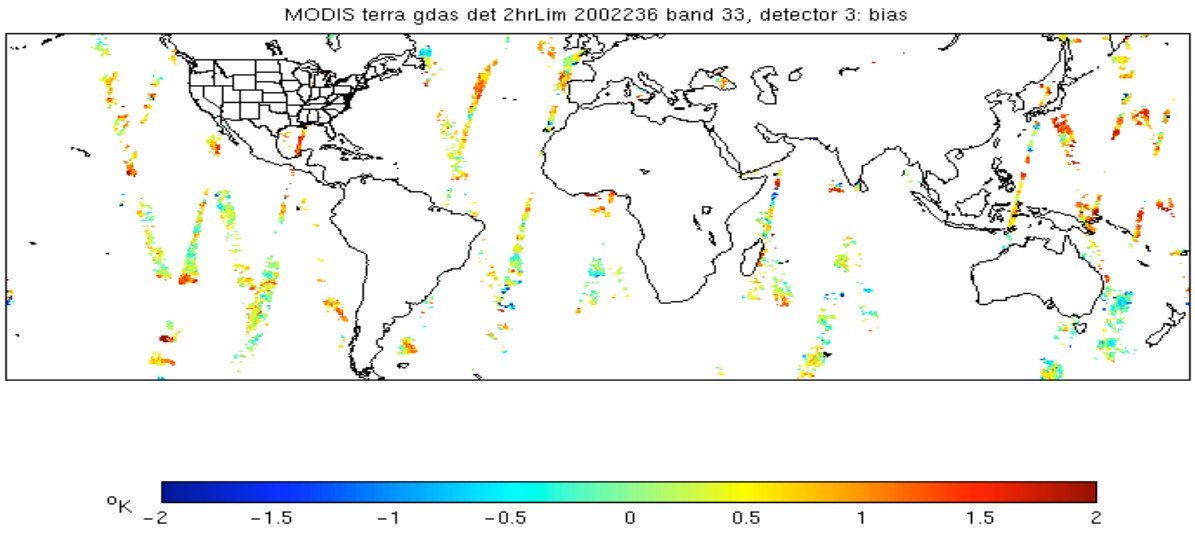

Figure SWS6. Global map of observed minus calculated BT bias (°K) for Terra MODIS band 33 (detector 3) on 24 Aug 2002 for clear, ocean scenes with zenith angle less than 20 degrees.

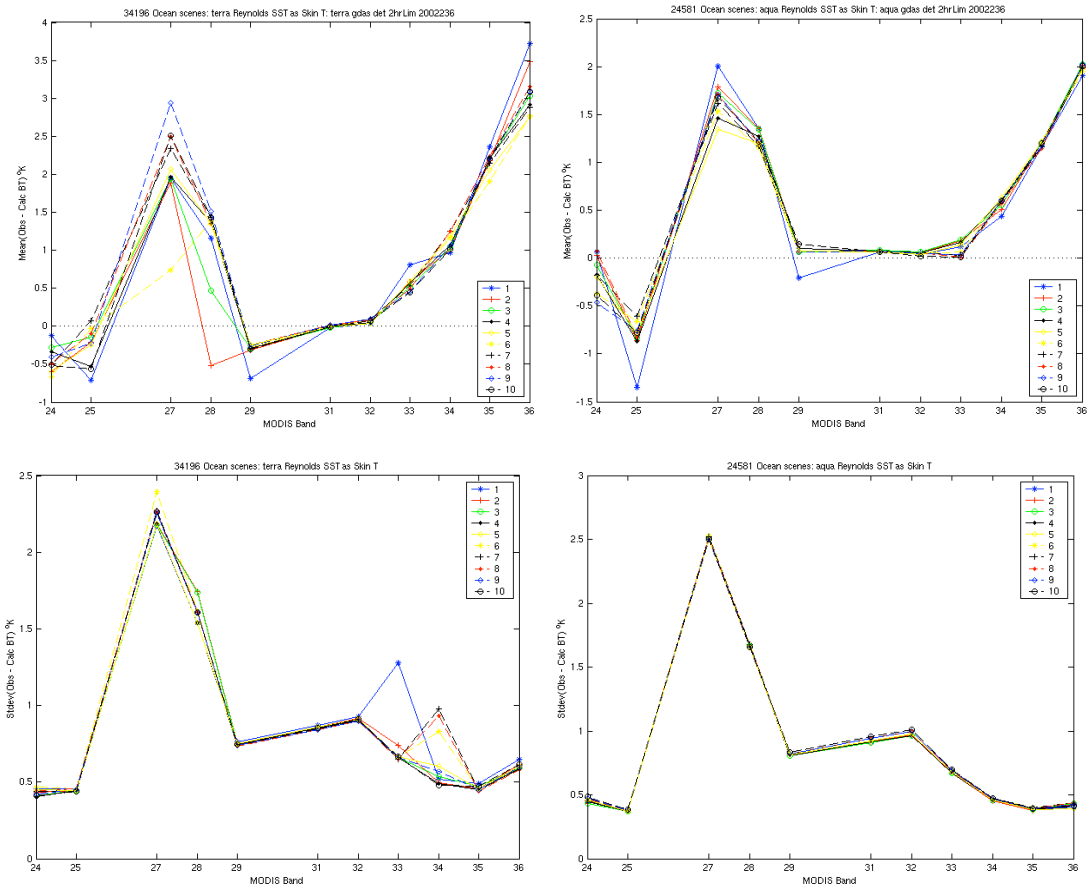

Figure SWS7. (top) Average global observed minus calculated BT by detector for MODIS bands 24, 25, 27, 28, 29, 31-36 for Terra (left) and Aqua (right). These averages highlight out-of-family detectors. (bottom) Standard deviation of global bias that highlights noisy detectors.

In addition to their utility in the MOD06 and MOD07 algorithms, detector-dependent global radiance bias calculations can be useful in identifying noisy or out-of-family detectors. By comparing the global average bias for each detector of a given band, outliers are easily identified (Figure SWS7 top row). In the same manner, a comparison of the standard deviation of the global bias of each detector can be used to identify noisy detectors that may not be (on average) out-of-family (Figure SWS7 bottom row). These comparisons were used to identify detectors to skip when performing the MOD07 retrieval in the new algorithm version.

Cloud top pressure algorithm, MOD06

To estimate the influence an atmospheric correction would have on the MOD06 cloud top pressure algorithm, a simulation was performed. The NCEP-GDAS temperature profile was compared with forward model-calculated 11 μm BT at each level (using only the profile above that level, setting surface pressure equal to the level, skin temperature equal to the temperature of the level, and emissivity equal to 1). The calculated 11 μm BT / GDAS Temperature comparison was expressed in terms of the amount that the cloud top pressure determination would change. Figure SWS8a shows the average simulation results for 77 cases at the SGP CART site, indicating that clouds at low levels in the atmosphere could see a change in MOD06 cloud pressure determination of 50hPa on average if the atmospheric correction were applied. Figure SWS8b shows a similar simulation for scenes in the moist tropical pacific. This indicates that by applying the atmospheric correction, for high sensor zenith angles, the cloud top pressure could change by up to 150 or 200 hPa. Even for near-nadir scenes, the effect could be as large as 100hPa for low clouds.

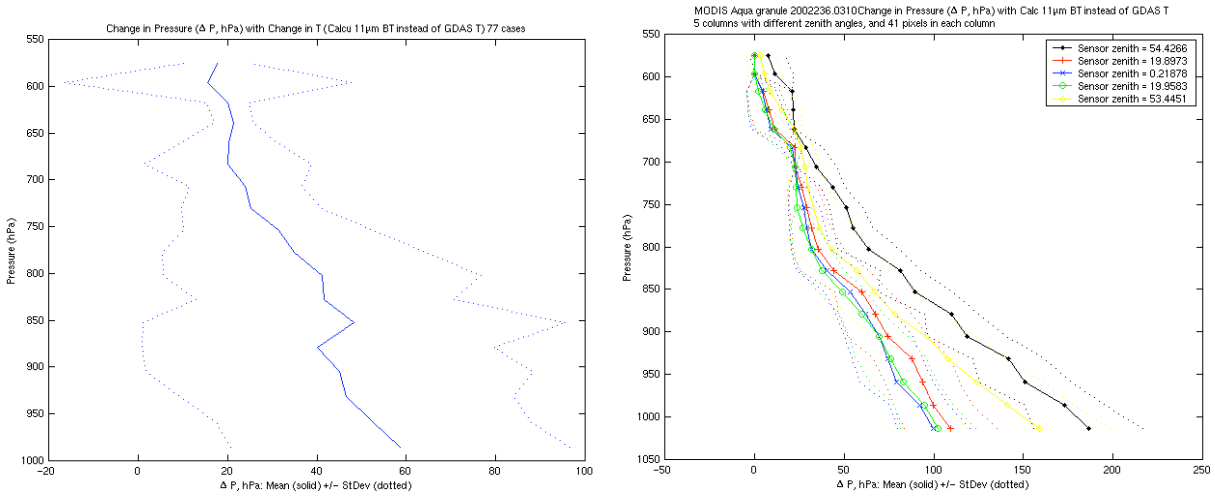

Figure SWS8: Simulated change in cloud-top pressure as determined by the MOD06 algorithm with the atmospheric correction as opposed to without. Left panel shows the average change in cloud top pressure by applying the atmospheric correction for 77 cases at the CART site distributed over all seasons. Right panel shows the same but for moist tropical scenes at varying sensor zenith angle. In both panels the dotted lines represent +/- one standard deviation from the mean (solid lines).

MODIS Cloud Top Properties (MOD06)

The CTP algorithm was modified by Hong Zhang to include moisture attention in the IR window height assignment; radiances calculated GDAS (Global Data Assimilation System) rather than temperatures are used to assign the height. A big improvement for low cloud heights was realized. Sea surface temperatures from the blended Reynolds SST and sea surface emissivity were tested for clouds over oceans, but no appreciable differences were noticed. The effect of noise level NEDR and radiance bias corrections are still being studied.

Low Cloud Top Properties

The IR window technique was adjusted to compare observed and GDAS calculated radiances (rather than observed brightness temperature and GDAS temperature profile); this includes an implicit correction for moisture attention in the atmospheric column. The new algorithm had an impact on clouds, lowering them by about 80 to 200 hPa. Figure HZ1 is the comparison of CTP before/after the IRW algorithm adjustment at 2130 24 Aug 2002 06:30 UTC on Aug. 24, 2002

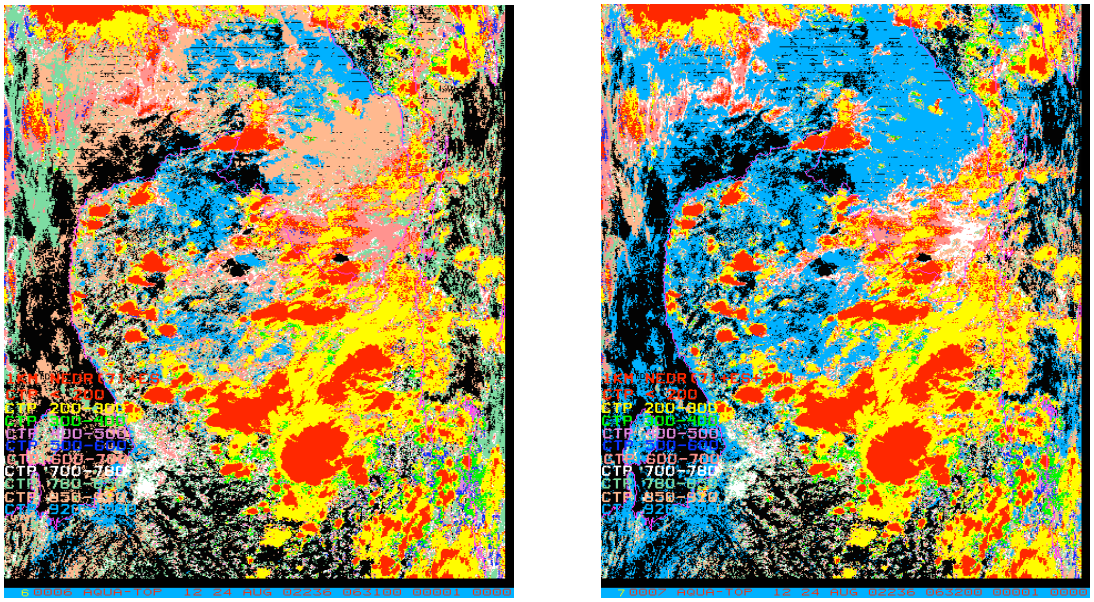

Figure HZ1: (left) IRW CTP without radiance profile correction and (right) IRW CTP with radiance profile correction for Aqua at 0630 UTC on 24 Aug 2002 in the northwestern Pacific.

NEDR and global bias correction

The threshold (NEDR) for using IRW rather than CO2 channel radiances for CTP determination was investigated along with the global detector-dependent radiance bias. The bias is the radiance from Aqua/MODIS observed minus calculated based on GDAS profiles and Reynolds SST. Figure HZ2 presents one of the case studies. The images show that (a) a small NEDR uses more CO2 slicing CTPs and (b) global bias corrections raise the clouds by 25 ~ 100 hPa. More investigations are underway to resolve these issues.

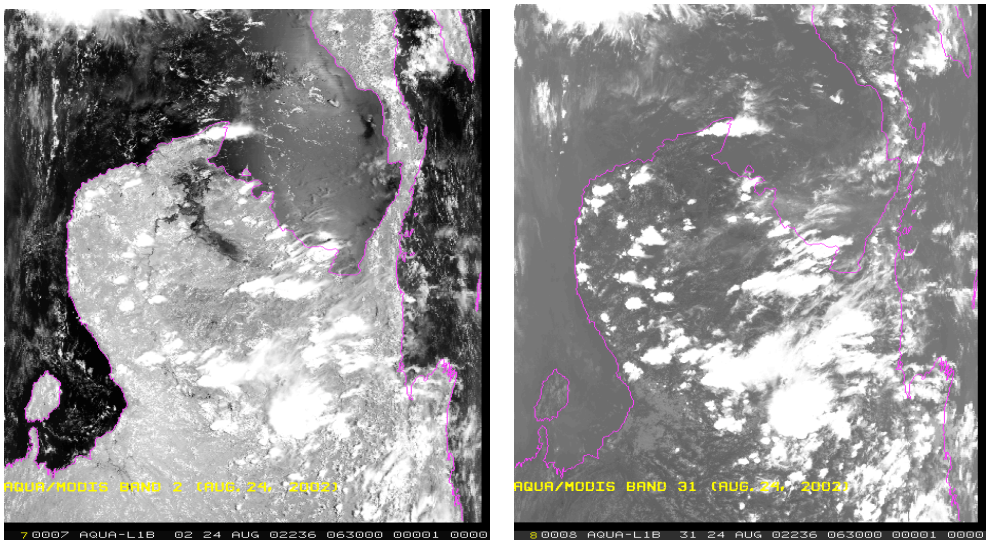

(a) Band 2 (b) Band 31

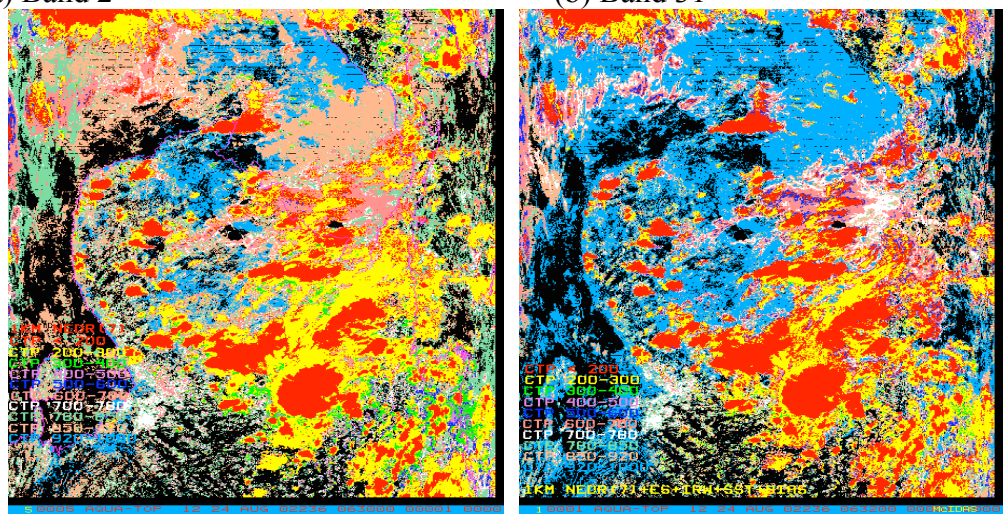

(c) CTP with NEDR(7) (d) CTP with NEDR(7) + IRW+SST+Bias

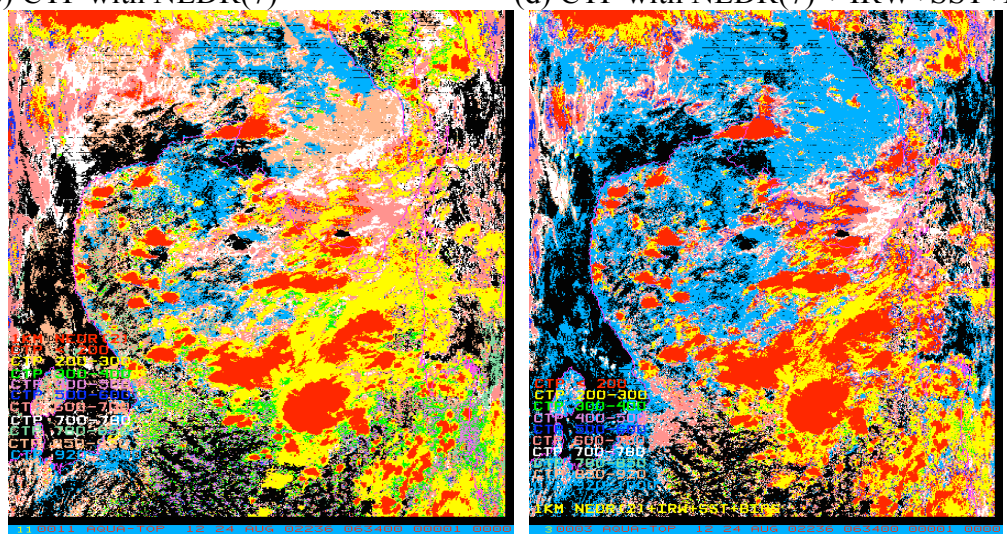

(e) CTP with small NEDR(2) (f) CTP with NEDR(2) + IRW+SST+Bias

Figure 4: Comparison of 1km resolution CTP for different combinations of NEDR and Bias.

AIRS subpixel cloud characterization using MODIS cloud products

The MODIS pixels with 1 km spatial resolution are being collocated within an AIRS footprint by Jun Li. Several collocation algorithms have been developed that are based on the scanning geometry of two instruments flown on the same satellite (Frey et al., 1995). The collocation algorithm should provide result with accuracy better than 1 km provided that the geometry information from both instruments is accurate. Then AIRS subpixel cloud properties can be characterized using the 1km MODIS cloud products such as classification mask, cloud phase mask. Figure JL2 shows a small study area within Figure JL1 (AIRS IR window brightness temperature images) of the MODIS cloud phase mask (left panel) and cloud classification mask (right panel) collocated (shading) to the AIRS footprints at 1920UTC on 06 September 2002. The ice and water clouds within AIRS footprints are well identified by the MODIS cloud phase mask. Some AIRS footprints contain mixed water clouds and ice clouds. From the right panel, single layer high clouds or low clouds with the AIRS footprints are well identified by the MODIS classification mask, some AIRS footprints contain multi-layer clouds (e.g., mid-level clouds and low clouds).

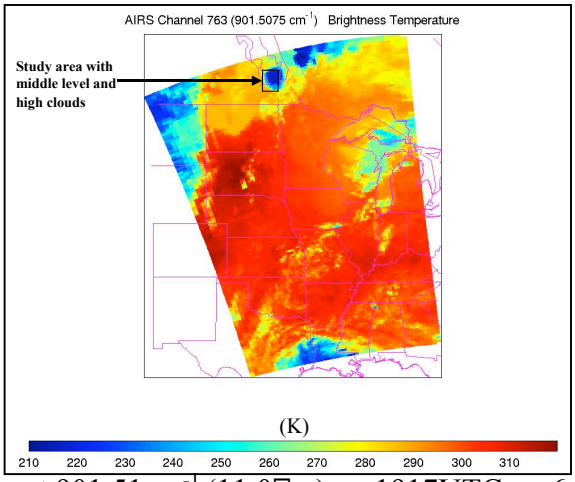

Figure JL1. The AIRS BT image at 901.51cm^{-1} (11.0□m) on 1917UTC on 6 September 2002.

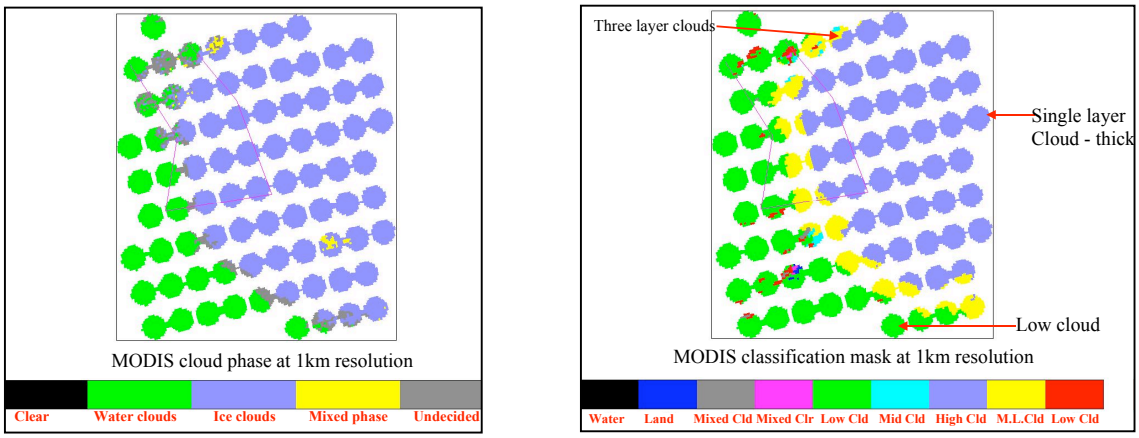

Figure JL2. MODIS cloud phase mask (left) and cloud classification mask (right) in the AIRS footprints within the study area (see Figure 1) at 1920UTC on 06 September 2002.

The MODIS classification mask is very important for determining how many cloud layers are actually contained in the AIRS footprint. Figure JL3 shows the AIRS clear footprints (blue), single layer cloud footprints (green), multi-layer cloud footprints (red) identified by the MODIS classification mask at 1920UTC on 06 September 2002. 55% of the AIRS footprints appear to be clear, 22% indicate single layer clouds, and approximately 23% are thought to be multi-layer clouds.

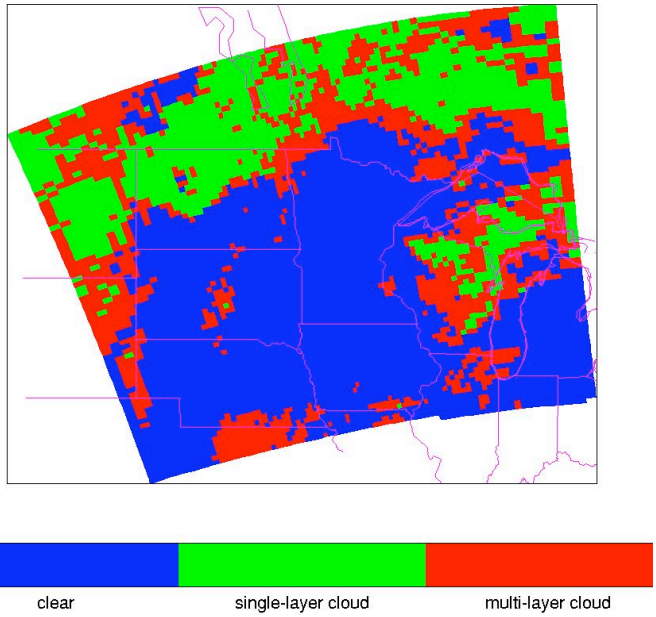

Figure JL3. The AIRS clear footprints (blue), single layer cloud footprints (green), multi-layer cloud footprints (red) identified by the MODIS classification mask at 1920UTC on 06 September 2002.

Synergistic use of MODIS cloud products and AIRS radiance measurements

In the MODIS/AIRS synergism, the MODIS cloud products such as CTP and ECA are used as the background and first guess information in the AIRS 1DVAR retrieval approach). The algorithm for cloud retrieval will be detailed in the separate paper (Li et al. 2003). Figure JL4 shows the MODIS 1 km classification mask collocated to the AIRS footprints over the southern Lake Michigan area at 1920UTC on 06 September 2002; a single layer thin cloud, determined by the MODIS classification mask, is selected for the cloud retrieval test. MODIS estimates the CTP to be 275 hPa. Figure JL5 shows the AIRS longwave clear BT calculation from ECMWF forecast analysis (black line), cloudy BT observation (red line), cloudy BT calculation from MODIS CTP and ECA (green line), and cloudy BT calculation from the AIRS 1DVAR retrieved CTP and ECA (blue line).

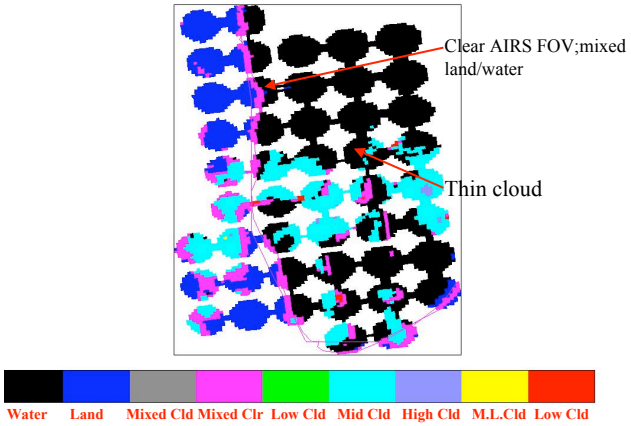

Figure JL4. The MODIS 1 km classification mask with the AIRS footprints over the Lake Michigan area at 1920UTC on 06 September 2002, showing a single layer thin cloud case.

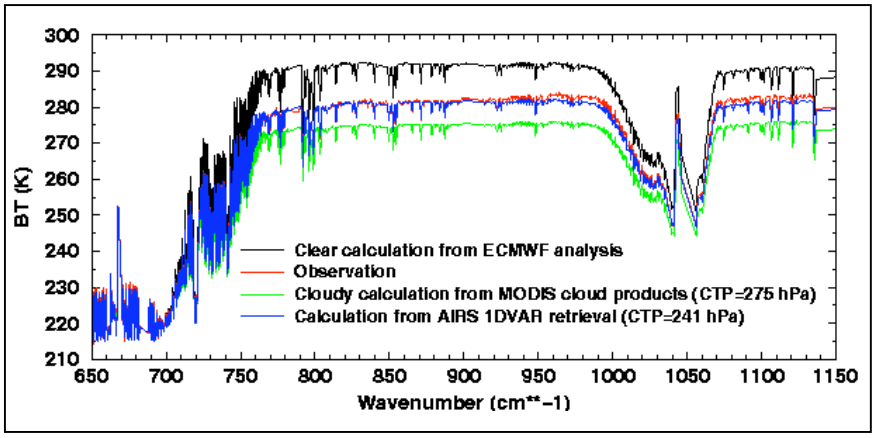

Figure JL5. The AIRS longwave clear BT calculation (black line), cloudy BT observation (red line), cloudy BT calculation (through cloudy radiative transfer model) from MODIS CTP and ECA (green line), and cloudy BT calculation from the AIRS 1DVAR retrieved CTP and ECA (blue line).

Figure JL6 shows the corresponding MODIS ECA (calculated from MODIS window spectral 11 and 12 m bands) and AIRS retrieved ECA spectra. From Figures JL5 and JL6 it can be seen that there is a difference between the AIRS cloudy BT calculation with MODIS cloud products (CTP and ECA) and the AIRS cloudy BT observation. However, after the 1DVAR retrieval, the AIRS cloudy BT calculation with AIRS retrieved cloud products (also CTP and ECA spectra) fits the cloudy observation very well. On one hand, AIRS raises the MODIS CTP by 34 hPa (from MODIS CTP 275 hPa to AIRS CTP 241 hPa), while on the other hand AIRS reduces the MODIS ECA by approximately 0.1 in this thin cloud case.

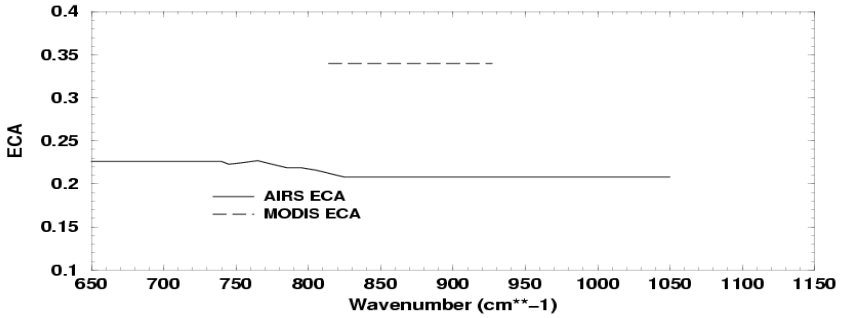

Figure JL6. The corresponding the MODIS ECA (constant for all MODIS spectral bands) and AIRS retrieved ECA spectra.

IMAPP Level 2 Products

IMAPP Level 2 science product Version 1.3 was released by Kathy Strabala in first quarter 2003. The release included updates to the cloud mask (MOD35) and cloud top property (MOD06CT) software that allows both Aqua and Terra data to be processed by the addition of a command line "platform" argument. This direct broadcast cloud mask release is concurrent with DAAC cloud mask operational MOD35 version 4.2.0; the cloud top properties and cloud phase release is concurrent with DAAC MOD06CT version 4.0.4. Quicklook direct readout IMAPP Level 2 products are now being routinely processed and placed on a web site at: http://cimss.ssec.wisc.edu/db_products/ . The purpose of this site is to allow users to quickly see what UW IMAPP products are available for the current atmospheric and surface conditions. All acquired Terra and Aqua passes are automatically remapped to a standard projection and combined together. Day and night overpasses are kept separately. An archive is also kept of images for the last several days. Products depicted on the web pages include true color, cloud mask, cloud top pressure, cloud phase and total precipitable water vapor. An example of a quick look day of true color UW Aqua overpasses is shown in Figure KIS1. Figure KIS2 is the cloud mask and total precipitable water vapor Level 2 products for the same day.

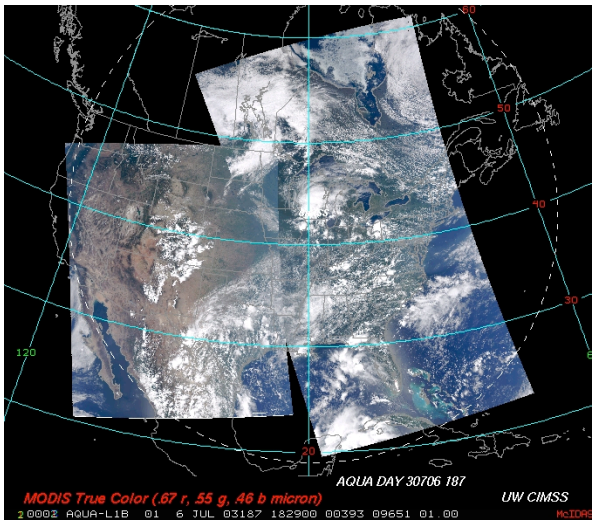

Figure KIS1. MODIS Aqua true color composite of overpasses collected on 6 July 2003.

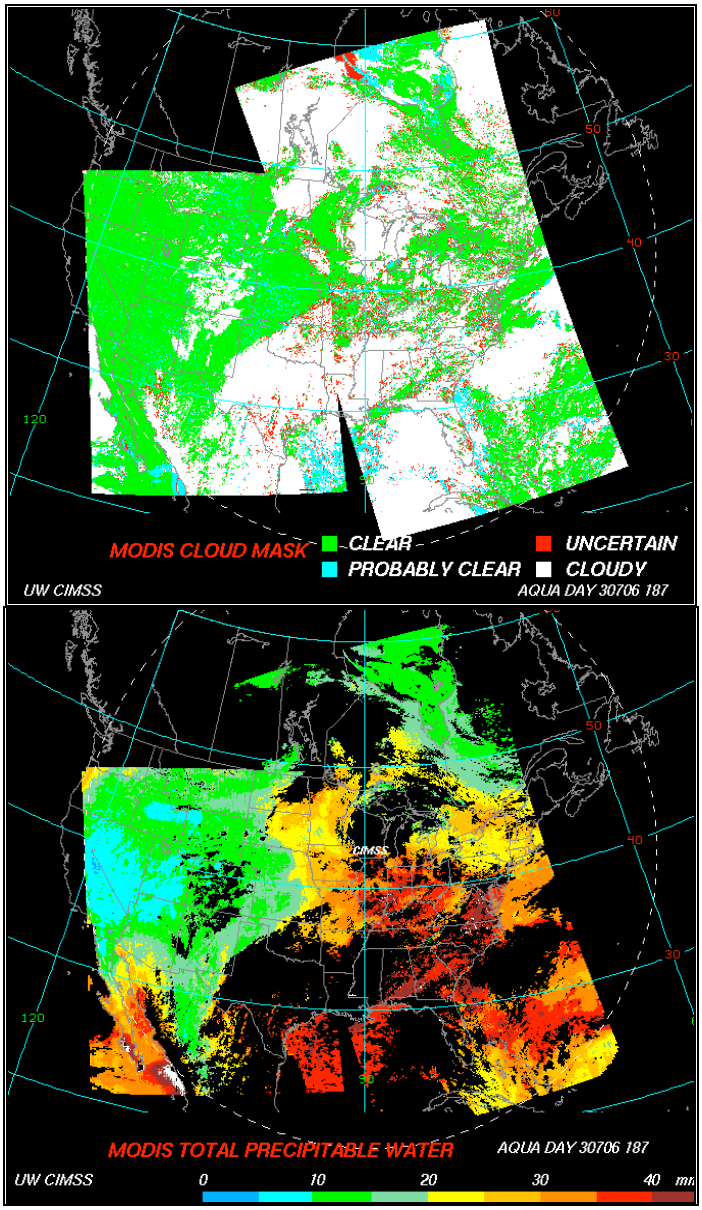

Figure KIS2. MODIS Aqua automated Level 2 science products processed from 6 July 2003 UW direct broadcast data. The top frame is the MODIS cloud mask (MYD35); the bottom frame is the total precipitable water vapor product (MYD07).

Automated Level 2 MODIS product generation in support of THORPEX

MODIS Aqua and Terra Level 2 science products were routinely produced using near real-time L1B data provided through the NOAA bent-pipe in support of THe Observing-system Research and Predictability EXperiment (THORPEX). Scripts were set up to execute IMAPP Level 2 production software as soon as new L1B data over the region of interest (Hawaii) were available. Cloud mask, cloud top property and atmospheric profiles products were generated and made

available to the THORPEX scientists through the UW visualization and manipulation toolkit McIDAS ADDE. Products were generated throughout the life of the experiment from mid-February through mid-March. The products have been archived and will be used to inter-compare with other satellite instruments as well as surface and ER-2 platform instruments.

MEETINGS / CONFERENCES

Richard Frey attended the Optical Remote Sensing of the Atmosphere Conference in Quebec City, Canada on Feb. 3-6, 2003. He presented a poster on "Cloud Detection from MODIS and AIRS".

Richard Frey attended the American Meteorological Society Annual Meeting in Long Beach, CA On Feb. 10-13, 2003 and presented a poster on "Comparisons of Regional and Global Cloud Products Between MODIS and Other Data Sets"

Chris Moeller participated in the THORpex field campaign in Hawaii in February and March, 2003 serving as ER-2 mission scientist.

Most of the UW MODIS team (Steve Ackerman, Bryan Baum, Richard Frey, Liam Gumley, Paul Menzel, Chris Moeller, Suzanne Wetzel Seemann) attended the MODIS Atmosphere Group Retreat in St. Michaels, MD on Mar. 17-19, 2003

Chris Moeller attended the MAS instrument meeting held May 20-21, 2003 and presented materials on MAS and SHIS calibration comparisons.

Richard Frey attended the Aqua Science Working Group Meeting at Goddard Space Flight Center, Greenbelt, MD on May 28-29, 2003 and presented a talk on "Operational MODIS Cloud Mask and Recent MODIS/AIRS Cloud Detection Comparison Studies"

Paul Menzel taught a ten day course on remote sensing with MODIS and AIRS in Maratea, Italy from 22 - 31 May 2003 at the invitation of the Consiglio Nazionale delle Ricerche (Italian National Council for Research).

PAPERS

Key, J., D. Santek, C.S. Velden, N. Bormann, J.-N. Thepaut, L.P. Riishojgaard, Y. Zhu, and W.P. Menzel, 2002, Cloud-drift and Water Vapor Winds in the Polar Regions from MODIS, *IEEE Trans. Geosci. Remote Sensing*, 41(2), 482-492.

King, M. D., W. P. Menzel, Y. J. Kaufman, D. Tanré, B. C. Gao, S. Platnick, S. A. Ackerman, L. A. Remer, R. Pincus, and P. A. Hubanks, 2003: Cloud and aerosol properties, precipitable water, and profiles of temperature and humidity from MODIS. IEEE Trans. Geosci. Remote Sens., **41**, 442-458.

Li., J., W.P. Menzel, Timothy J. Schmit, Fengying Sun, James Gurka, AIRS sub-pixel cloud characterization using MODIS cloud products, submitted to *Journal of Applied Meteorology*.

Liu, Y. and J. Key, 2002, Detection and analysis of clear sky, low-level atmospheric temperature inversions with MODIS, *J. Atmos. Ocean. Tech*., accepted (June 2003).

Moeller, C. C., H. E. Revercomb, S. A. Ackerman, W. P. Menzel, and R. O. Knuteson, Evaluation of MODIS thermal IR band L1B radiances during SAFARI 2000, *J. Geophys. Res.*, 108(D13), 8494, doi:10.1029/2002JD002323, 2003.

Platnick, S., M. D. King, S. A. Ackerman, W. P. Menzel, B. A. Baum, J. C. Riédi, and R. A. Frey, 2003: The MODIS cloud products: Algorithms and examples from Terra. IEEE Trans. Geosci. Remote Sens., **41**, 459-473.

Seemann, S. W., J. Li., W.P. Menzel, and L.E. Gumley, 2003: "Operational retrieval of atmospheric temperature, moisture, and ozone from MODIS infrared radiances." Accepted by Journal of Applied Meteorology. In press.

Conference Papers:

Liu, Y. and J. Key, 2003, Study of clear sky, low-level atmospheric temperature inversions using satellite data, *Proceedings of the Seventh Conference on Polar Meteorology and Oceanography*, American Meteorological Society, Hyannis, MA, May 12-16.

Moeller, C. C., R. O. Knuteson, D. Tobin, H. E. Revercomb, and W. P. Menzel, 2003, Assessment of Aqua MODIS and AIRS TIR band L1B radiances using ER-2 based observations during TX-2002. EOS VII conference, SPIE Annual Mtg., Aug 3-6, 2003, San Diego.

Santek, D., J. Key, and C. Velden, 2003, Real-time Derivation of Cloud Drift and Water Vapor Winds in the Polar Regions from MODIS Data, *Proceedings of the 12th Conf. on Satellite Meteorology and Oceanography*, American Meteorological Society, Long Beach, CA, 9-13 February 2003.